

Review

The Latest FDA-Approved Pharmaceuticals Containing Fragments of Tailor-Made Amino Acids and Fluorine

Qian Wang¹, Jianlin Han^{1,*}, Alexander Sorochinsky^{2,*}, Aitor Landa³, Greg Butler⁴
and Vadim A. Soloshonok^{3,5,*}

¹ Jiangsu Co-Innovation Center of Efficient Processing and Utilization of Forest Resources, College of Chemical Engineering, Nanjing Forestry University, Nanjing 210037, China

² V.P. Kukhar Institute of Bioorganic Chemistry and Petrochemistry, The National Academy of Sciences of Ukraine, 1 Murmanska Str., 02094 Kyiv, Ukraine

³ Department of Organic Chemistry I, Faculty of Chemistry, University of the Basque Country UPV/EHU, Paseo Manuel Lardizábal 3, 20018 San Sebastián, Spain

⁴ Oakwood Chemical, Inc., 730 Columbia Hwy. N, Estill, SC 29918, USA

⁵ IKERBASQUE, Basque Foundation for Science, Alameda Urquijo 36-5, Plaza Bizkaia, 48011 Bilbao, Spain

* Correspondence: hanjl@njfu.edu.cn (J.H.); sorochinsky.a@gmail.com (A.S.); vadym.soloshonok@ehu.eus (V.A.S.)

Abstract: Nowadays, the selective introduction of fluorine into bioactive compounds is a mature strategy in the design of drugs allowing to increase efficiency, biological half-life and bio-absorption. On the other hand, amino acids (AAs) represent one of the most ubiquitous classes of naturally occurring organic compounds, which are found in over 40% of newly marketed small-molecule pharmaceutical drugs and medical formulations. The primary goal of this work is to underscore two major trends in the design of modern pharmaceuticals. The first is dealing with the unique structural characteristics provided by the structure of amino acids featuring an abundance of functionality and the presence of a stereogenic center, all of which bodes well for the successful development of targeted bioactivity. The second is related to fine-tuning the desired activity and pharmacokinetics by selective introduction of fluorine. Historically, both trends were developed separately as innovative and prolific approaches in modern drug design. However, in recent decades, these approaches are clearly converging leading to an ever-increasing number of newly approved pharmaceuticals containing both structural features of amino acids and fluorine.

Keywords: pharmaceuticals; tailor-made amino acids; fluorine; drug design; asymmetric synthesis



Citation: Wang, Q.; Han, J.; Sorochinsky, A.; Landa, A.; Butler, G.; Soloshonok, V.A. The Latest FDA-Approved Pharmaceuticals Containing Fragments of Tailor-Made Amino Acids and Fluorine. *Pharmaceuticals* **2022**, *15*, 999. <https://doi.org/10.3390/ph15080999>

Academic Editor: Chung-Shan Yu

Received: 19 July 2022

Accepted: 11 August 2022

Published: 14 August 2022

Publisher's Note: MDPI stays neutral with regard to jurisdictional claims in published maps and institutional affiliations.



Copyright: © 2022 by the authors. Licensee MDPI, Basel, Switzerland. This article is an open access article distributed under the terms and conditions of the Creative Commons Attribution (CC BY) license (<https://creativecommons.org/licenses/by/4.0/>).

1. Introduction

Pharmaceutical drugs enjoy a tremendously wide range of molecular architectures and chemical functionalities. Nevertheless, the structural analysis allows discerning some general trends guiding the rational design of modern pharmaceuticals. One of these growing trends is the use of amino acid (AA) residues [1–6] and related compounds, such as diamines and amino alcohols. AAs represent one of the most ubiquitous classes of naturally occurring compounds serving prolific biological functions [7]. Thus, the inclusion of an AA, or its derivative, in a drug candidate amplifies functional and structural complexity by providing two orthogonal functional amino and carboxyl groups. These aspects usually bode well for the success rate of molecules moving from the discovery phase to the market [8–12]. Another rapidly growing trend in the design of modern drugs is the introduction of fluorine-containing substituents into the structure of a drug candidate [13–16]. Selective fluorination allows for fine-tuning of the targeted bioactivity and pharmacokinetics. Over the last 20 years, fluorine scanning and editing became rather standard steps in the design of new drugs [17–21].

In the present review article, we profile the eleven selected drugs approved by the FDA in 2021 (Figure 1), which contain the fragment of amino acid and six of them feature fluorine.

In particular, we will discuss the following drugs containing both AA residue and fluorine: Scemblix (1), Tavneos (2), Qulipta (3), Lumakras (4), Pepaxto (5), and Cabenuva (6). The rest of these compounds we are going to profile contain only AA residues, which include Korsuva (7), Bylvay (8), Brexafemme (9), Azstarys (10), and Cytalux (11). Therapeutic areas of the compounds 1–11 include cancer (1,4,5,11), autoimmune disease (2), migraine (3), HIV (6), kidney disease (7), skin disease (8), vaginal disease (9) and attention deficit hyperactivity disorder (10). For each of these 11 compounds, we will discuss biological properties and detailed synthesis. In the case of fluorinated molecules (1–6), we will also discuss the effect of fluorine introduction and the source of fluorinated materials.

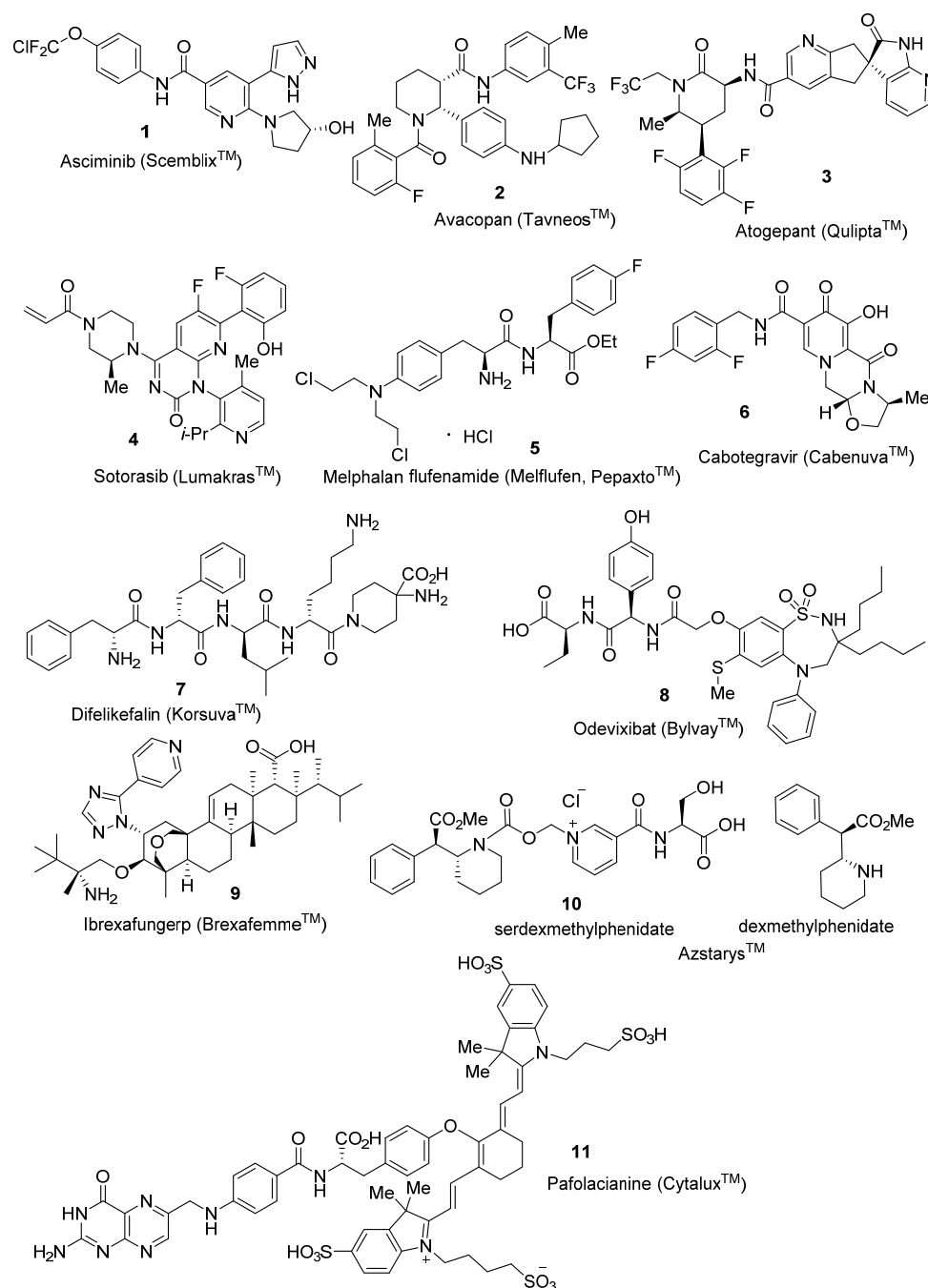


Figure 1. Structures of drugs 1–11.

2. Asciminib (Scemblix™)

Asciminib **1** is an allosteric inhibitor of the tyrosine kinase activity of the BCR-ABL1 oncoprotein which causes chronic myelogenous leukemia [22]. In contrast to tyrosine kinase inhibitors interacting with the ATP-binding site of BCR-ABL1, asciminib **1** binds to the myristoyl-binding pocket on protein affording high selectivity for inhibition of BCR-ABL1 kinase. Because asciminib **1** does not bind to the ATP-binding site it retains activity against BCR-ABL1 mutations which are associated with acquired resistance toward ATP-competitive drugs [23]. The US FDA approved asciminib **1** as an oral drug for the treatment of adults with Philadelphia chromosome-positive (Ph+) chronic myeloid leukemia and Philadelphia chromosome-positive (Ph+) acute lymphoblastic leukemia in 2021 [24]. This drug may also treat non-malignant diseases associated with abnormally activated ABL1 kinase enzyme [25,26].

The X-ray crystal structure analysis of compound **12** (Figure 2) bound to the ABL1 protein showed that the CF₃O-group [13,27] is located in the deepest part of the myristate pocket and one of the fluorine atoms highly interacts with the carbonyl carbon of leucine-359 [28]. Further molecular modeling study indicated that replacing one of the fluorine atoms with chlorine leads to a slightly larger ClCF₂O-group which can easily be placed in the myristate pocket. This modification improves the activity of compound **13** in biochemical and cellular assays for ABL1 kinase inhibition compared to the CF₃O-counterpart **12**. Replacing the pyrimidine ring of **13** with a pyrazole ring only slightly reduced the cellular activity of asciminib **1**. However, its hERG activity was markedly reduced. The introduction of an additional hydroxyl group in the pyrrolidine ring of **12** increased the solubility but decreased the cellular activity of **14**.

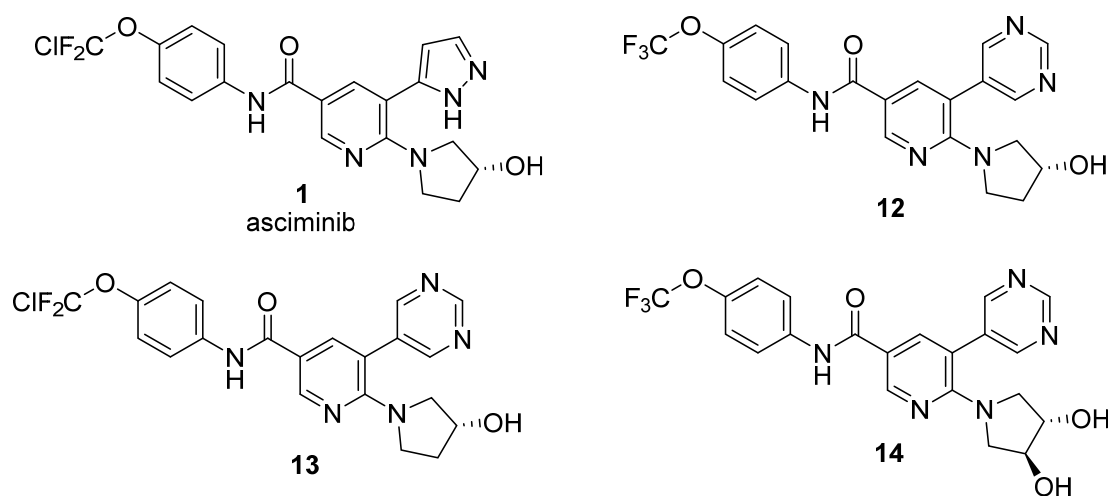
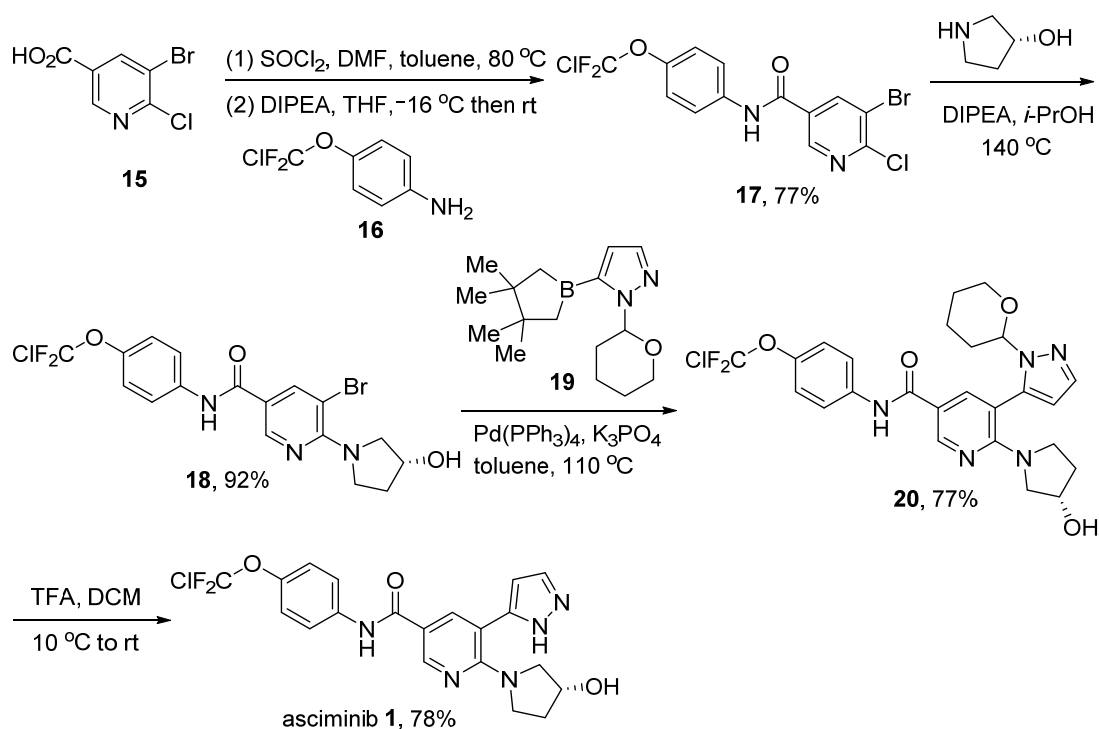


Figure 2. Structure of asciminib **1** and its analogs.

The synthesis of asciminib **1** starts from 5-bromo-6-chloronicotinic acid **15** and 4-(chlorodifluoromethoxy)aniline **16** (Scheme 1) [28]. It should be noted that **16** derivative is commercially available and can be obtained according to the described procedures [29]. The acid chloride derived from acid **15** was condensed with the aniline **16** in the presence of *N,N*-diisopropylethylamine (DIPEA) at room temperature to obtain nicotinamide **17** in 77% yield. S_NAr displacement of the chlorine atom of **17** by treatment with the enantiomerically pure (*R*)-pyrrolidin-3-ol in the presence of DIPEA at 140 °C afforded the amine **18**. Subsequently, amine **18** was subjected to a Suzuki–Miyaura coupling with tetrahydropyran-2-yl protected (1*H*-pyrazol-5-yl)boronic acid **19** under Pd(PPh₃)₄ catalysis at 110 °C providing the protected pyrazole **20** in good yield. Finally, deprotection of tetrahydropyran group with TFA at 10–25 °C gave asciminib **1** in 47% yield over four steps.



Scheme 1. Synthesis of asciminib 1.

3. Avacopan (Tavneos™)

Avacopan **2** is an orally bioavailable and highly selective antagonist of human C5aR1 which was developed by ChemoCentryx [30]. The complement anaphylatoxin C5a is a potent inflammatory mediator and exerts its effects by interacting with the C5a receptor 1 (C5aR1) on the surface of neutrophils controlling cell activation and migration [31]. The C5a ligand and its receptor C5aR1 play a central role in the pathogenesis of anti-neutrophil cytoplasmic antibody (ANCA)-associated vasculitis which is characterized by blood vessel inflammation resulting in tissue destruction [32,33]. The US FDA approved avacopan **2** for the treatment of ANCA-associated vasculitis, which is a rare autoimmune disease, in 2021 [30,34].

From the structural point of view, avacopan **2** contains fluorine atom and trifluoromethyl group bounded to different aromatic rings which improves C5aR1 inhibition ($\text{IC}_{50} < 5\text{ nM}$) compared with chlorinated counterparts **21** and **22** ($\text{IC}_{50} > 5\text{ nM}$) (Figure 3) [35,36].

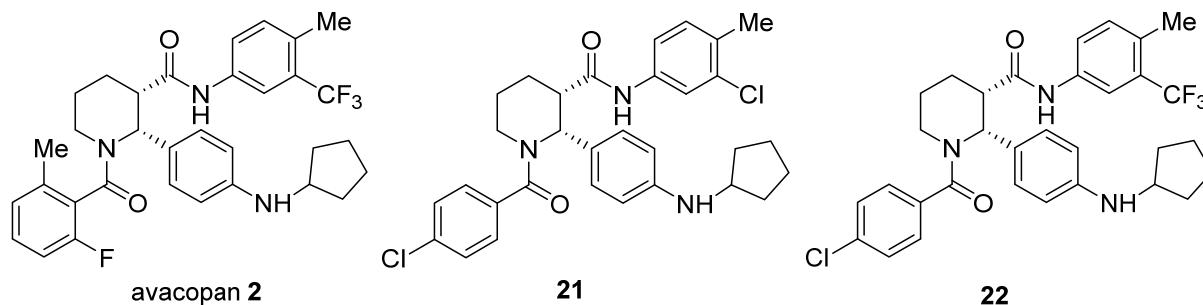
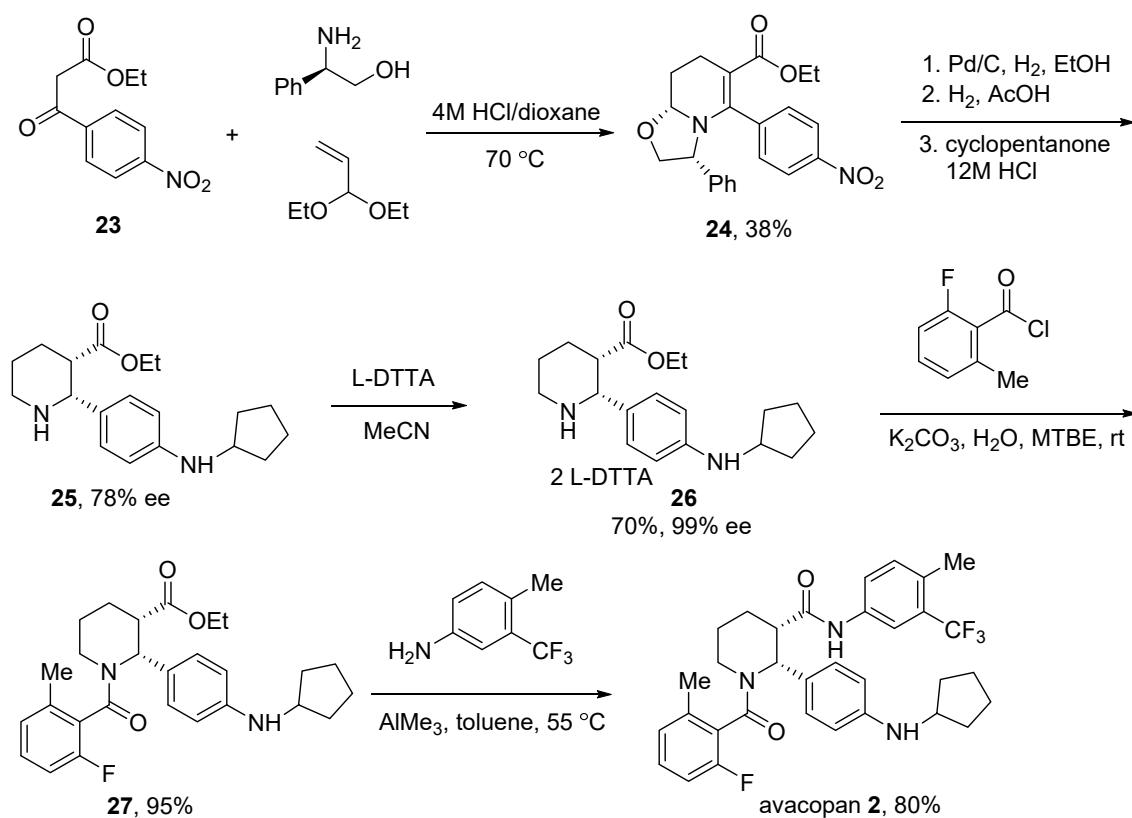


Figure 3. Structures of avacopan 2 and its analogs.

The synthesis of avacopan **2** starts from three-component condensation of ketoester **23**, (*R*)-2-amino-2-phenylethan-1-ol and acrolein diethyl acetal in the presence of catalytic HCl, which gave the bicyclic tetrahydropyridine derivative **24** in 38% yield. Hydrogenation of **24** on 10% Pd/C in ethanol proceeded with good *cis*-diastereoselectivity. The following reduction of the nitro group, reductive removal of the chiral auxiliary and reductive amination of the deprotected piperidine intermediate with cyclopentanone afforded the amino acetate **25** with 78% ee. Chiral resolution [37,38] of **25** by treatment with di-*p*-toluoyl-L-tartaric acid (L-DTTA) in acetonitrile provided di-tartaric salt **26** in 70% yield and 99% ee. Benzoylation of the piperidine nitrogen of **26** with 2-fluoro-6-methylbenzoyl chloride gave amide **27**. Finally, the synthesis of avacopan **2** was conveniently achieved using AlMe₃-mediated direct coupling of the ester group of **27** and 4-methyl-5-trifluoromethylaniline in good yield (80%) after recrystallization from ethanol/water (Scheme 2).



Scheme 2. Synthesis of avacopan **2**.

4. Atogepant (Qulipta™)

Atogepant **3** is developed by AbbVie as an orally active and selective antagonist of the calcitonin gene-related peptide (CGRP) receptors [39]. CGRP is a neuropeptide widely distributed in the central and peripheral nervous system and regulates cardiac excitability, microvascular permeability, vascular smooth muscle tone, and angiogenesis. CGRP acts by binding to specific cell surface receptors preferentially activating adenylate cyclase [40]. Recently, it was shown that CGRP levels correlate with migraine attacks and CGRP receptors are expressed in the brain regions associated with migraine pathophysiology [41]. Therefore, CGRP receptor antagonists, such as clinical agents atogepant **3**, ubrogepant **28**, and rimegepant **29** (Figure 4), also called gepants, were developed for the treatment of acute migraine headache [42]. The US FDA approved atogepant **3** for the preventive treatment of episodic migraine in adults in 2021 [43].

Atogepant **3** is a polycyclic compound, containing 2-azaspiro[4.4]nonan unit in (*S*) configuration. The spiroazaindane unit is linked with an amide bond to a piperidine-2-one ring bearing 6-(*R*)-methyl and 5-(*R*)-2,3,6-trifluorophenyl substituents. These fluorine substituents provide an increase in atogepant **3** binding affinity for the receptor compared with ubrogepant **28**, which contains an unsubstituted phenyl ring. At the same time, 2,2,2-trifluoroethyl group at the nitrogen atom of piperidine-2-one ring improves the potency and bioavailability of atogepant **3**. While atogepant **3** and ubrogepant **28** contain an aromatic linker, piperidine linker is present in rimegepant **29**.

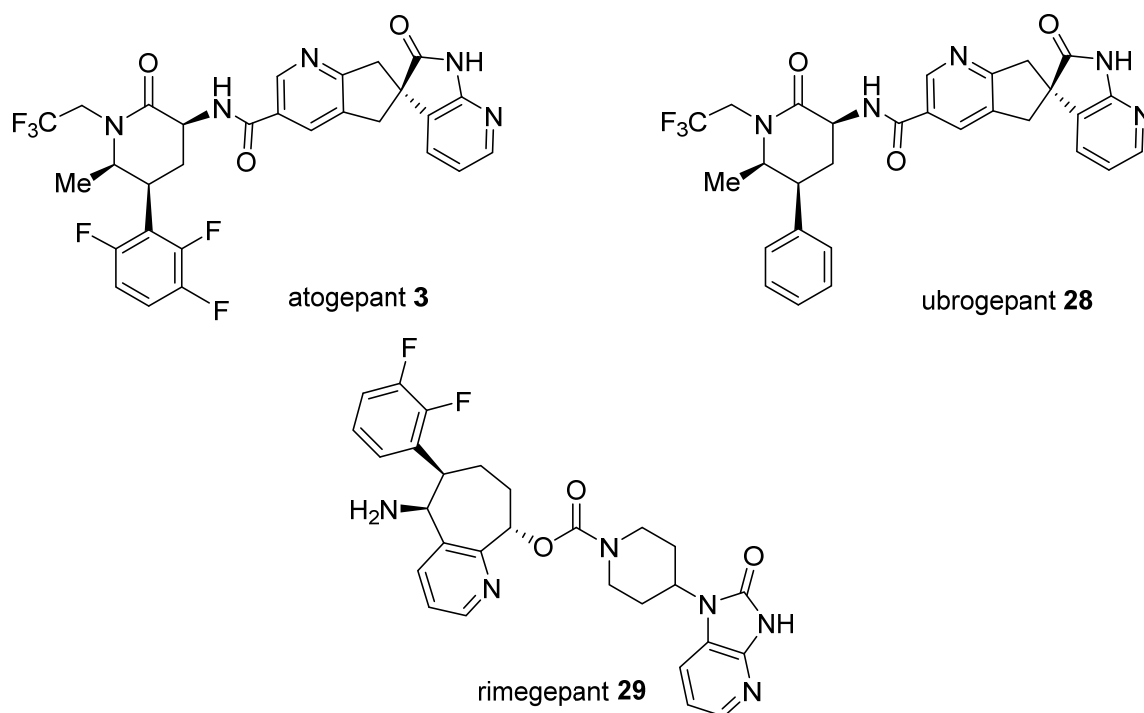
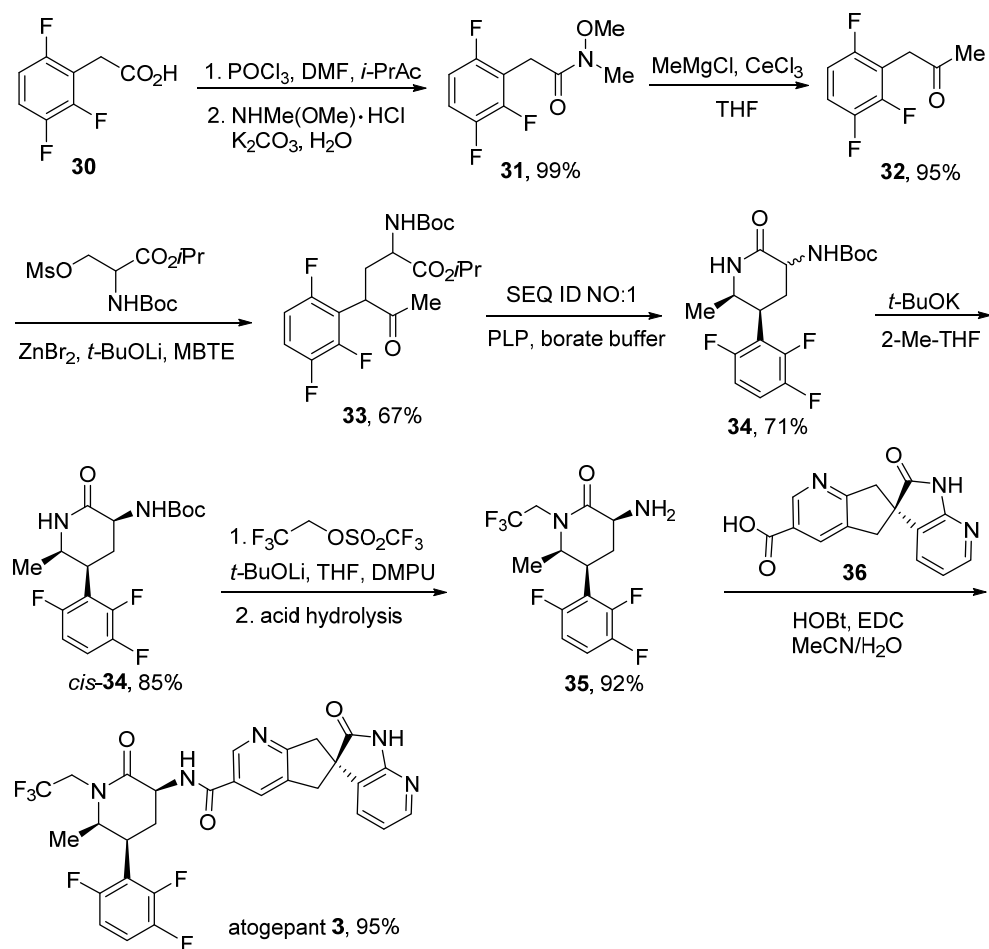


Figure 4. Structures of atogepant **3**, ubrogepant **28**, and rimegepant **29**.

The synthesis of atogepant **3** (Scheme 3) was carried out using fluorinated 2-phenylacetic acid **30** as a starting material [44,45]. Acid **30** was treated with POCl_3 in isopropyl acetate (*i*-PrAc) at 0 °C and then acid chloride was condensed with *N,O*-dimethylhydroxylamine hydrochloride in the presence of K_2CO_3 to yield *N*-methoxy-*N*-methylamide **31** in excellent yield. The conversion of amide **31** into ketone **32** was readily accomplished by treatment with methylmagnesium chloride/cerium(III) chloride in THF. The ketone **32** was alkylated using *N*-(*tert*-butoxycarbonyl)-*O*-(methylsulfonyl)serin isopropyl ester under basic conditions to provide keto ester **33** as one pair of diastereomers. The dynamic kinetic resolution [46,47] of keto ester **33** applying ω -transaminase with pyridoxal 5'-phosphate (PLP) as cofactor provided piperidin-2-one **34** high diastereoselectivity at positions C5 and C6. Treatment of crude *cis/trans* mixture **34** with *t*-BuOK in 2-Me-THF provided crystalline *cis*-**34**. *N*-Trifluoroethylation of piperidine-2-one of *cis*-**34** with trifluoroethyl trifluoromethanesulfonate followed by removal of Boc group generated the 3-aminopiperidin-2-one **35** in 92% yield. Coupling of **35** with carboxylic acid **36** in the presence of 1-hydroxybenzotriazole (HOBt) and 1-(3-dimethylaminopropyl)-3-ethylcarbodiimide hydrochloride (EDC) at room temperature gave atogepant **3** in 95% yield as a monohydrate. An alternative method for synthesis of the key 3-aminopiperidin-2-one intermediate **35** including the separation of the racemic mixture of **34** by chiral-HPLC was also described [44].



Scheme 3. Synthesis of atogepant 3.

5. Sotorasib (Lumakras™)

Sotorasib 4 is developed by Amgen as a RAS GTPase family inhibitor [48]. Among members of the RAS family of proteins, the KRAS isoform is the most frequently mutated oncogene in cancer and mutations mostly occur in codon 12, such as p.G12D (41%), p.G12V (28%), and p.G12C (14%) [49]. The KRAS protein functions as a signaling molecule capable of subsequent regulation of the proliferation by alternating between a guanosine diphosphate-bound inactive form and a guanosine triphosphate-bound active form. Recently, a series of quinazolinone derivatives were identified as selective covalent inhibitors of KRAS^{G12C} interacting with the cryptic pocket on the surface of the mutated protein [50]. The US FDA approved sotorasib 4 in 2021 for the treatment of adult patients, with KRAS^{G12C}-mutated locally advanced or metastatic non-small cell lung cancer (NSCLC) and colorectal cancer, who have received at least one prior systemic therapy [51].

Sotorasib 4 contains a pyrido[2,3-*d*]pyrimidin-2(1*H*)-one unit substituted with 4-methyl-2-(propan-2-yl)pyridin-3-yl, (2*S*)-2-methyl-4-(prop-2-enyl)piperazin-1-yl, 2-fluoro-6-hydroxyphenyl, and fluoro groups. 2,6-Dialkyl substituents on the pyridine ring constrain biaryls' rotation around the C-N bond affording the stable atropisomer. Sotorasib 4 contains two fluorine atoms on different aromatic rings and replacing the chloro substituent of compound 37 for fluorine increases bioavailability, although a modest loss of activity in cellular assays is observed (Figure 5) [52].

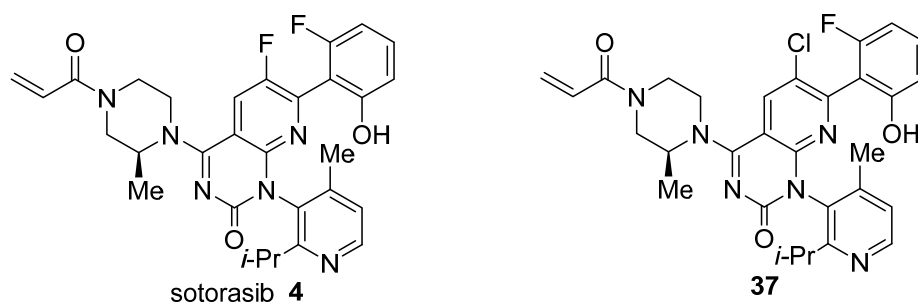
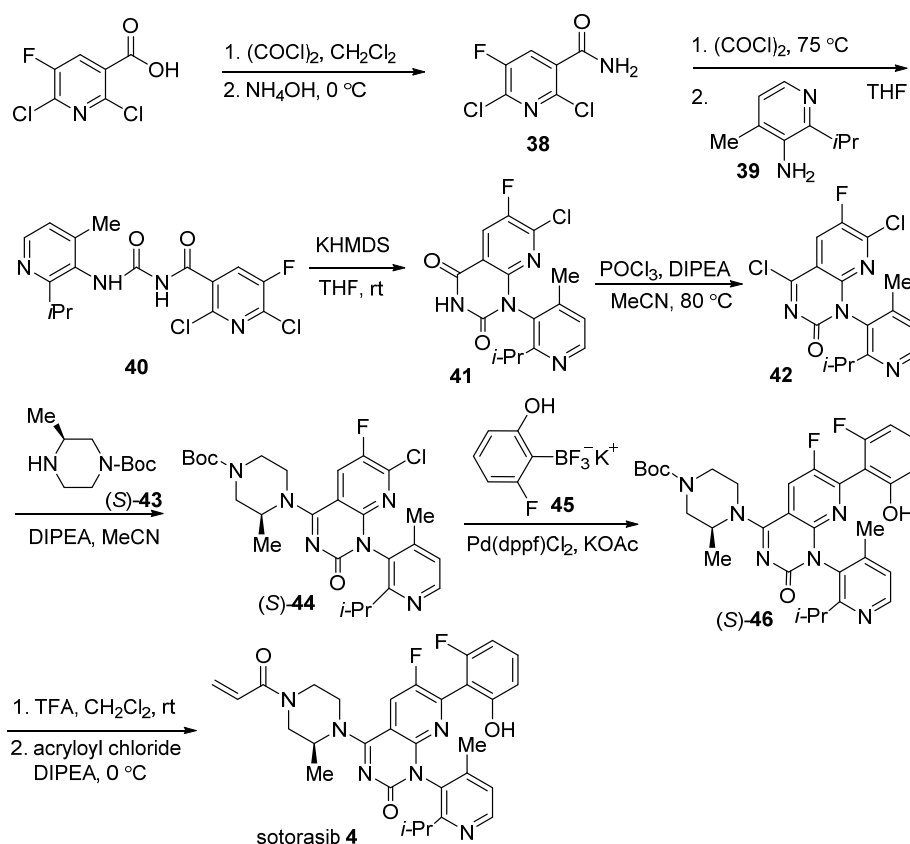


Figure 5. Structure of sotorasib 4 and its analog 37.

Multi-step synthesis of sotorasib **4** starts from commercial 2,6-dichloro-5-fluoronicotinic acid (Scheme 4) [53]. The first step consisted of its treatment with oxalyl chloride in CH_2Cl_2 providing corresponding acid chloride, which directly reacted with ammonium hydroxide solution in dioxane at 0°C to give nicotinamide **38**. The reaction of **38** with oxalyl chloride in THF at 75°C followed by the addition of aminopyridine **39** gave urea **40**. Cyclization of **40** by treatment with potassium hexamethyldisilazide in THF at room temperature afforded **41** after chromatography purification on silica gel. Chlorination of **41** with POCl_3 in the presence of DIPEA in acetonitrile at 80°C afforded **42**, which without purification underwent nucleophilic substitution with BOC-protected piperazine **43** to yield **44**. The Suzuki–Miyaura reaction between **44** and potassium trifluoroborate **45** in the presence of $\text{PdCl}_2(\text{dppf})\cdot\text{CH}_2\text{Cl}_2$ complex and potassium acetate at 90°C gave the coupling product **46**. Finally, sotorasib **4** was obtained by Boc deprotection with TFA; reaction with acryloyl chloride in the presence of DIPEA, and purification by silica gel chromatography.



Scheme 4. Synthesis of sotorasib 4.

6. Melphalan Flufenamide (Melflufen, Pepaxto™)

Melphalan flufenamide **5** is an ethyl ester of a lipophilic dipeptide combining melphalan and *L-p*-fluorophenylalanine and developed by Oncopeptides for the treatment of multiple myeloma and amyloid light-chain amyloidosis. The highly lipophilic melphalan flufenamide penetrates cell membranes and is hydrolyzed in aminopeptidase-positive tumor cells by peptidases and esterases to yield hydrophilic cytotoxic alkylating agents, such as melphalan **47** and desethyl melphalan flufenamide **48** (Figure 6). This results in irreversible DNA damage, apoptosis, and cell death [54]. Melphalan flufenamide **5** shows antitumor activity in multiple myeloma, lymphoma and acute myeloid leukemia cell lines, and primary tumor cells [55]. The application of Melphalan flufenamide **5** enhances efficacy and reduces toxicity compared to melphalan **47**. Structure-activity relationship (SAR) analysis for melphalan-containing dipeptide derivatives **49–51** shows similar cytotoxic activity but lower metabolic stability in comparison with melphalan flufenamide **5** [56]. The US FDA approved melphalan flufenamide **5** in combination with dexamethasone for the treatment of pre-treated adult patients with relapsed or refractory multiple myeloma in 2021 [57].

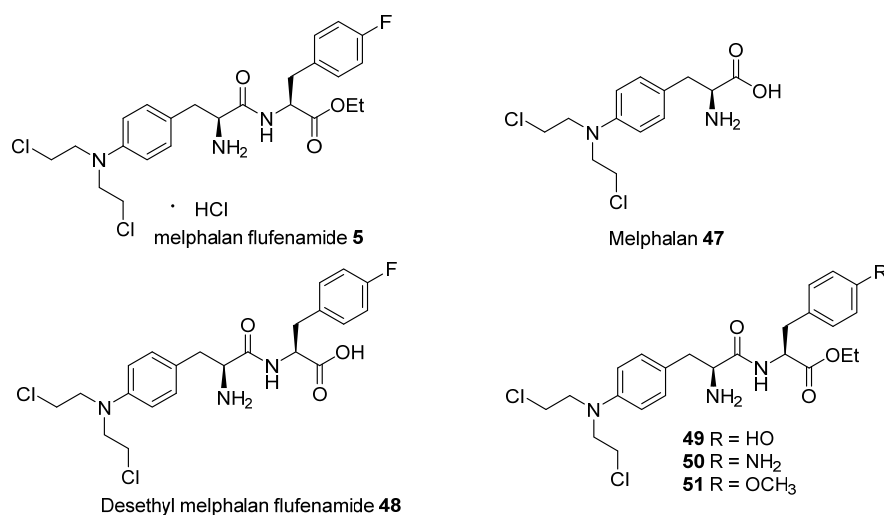
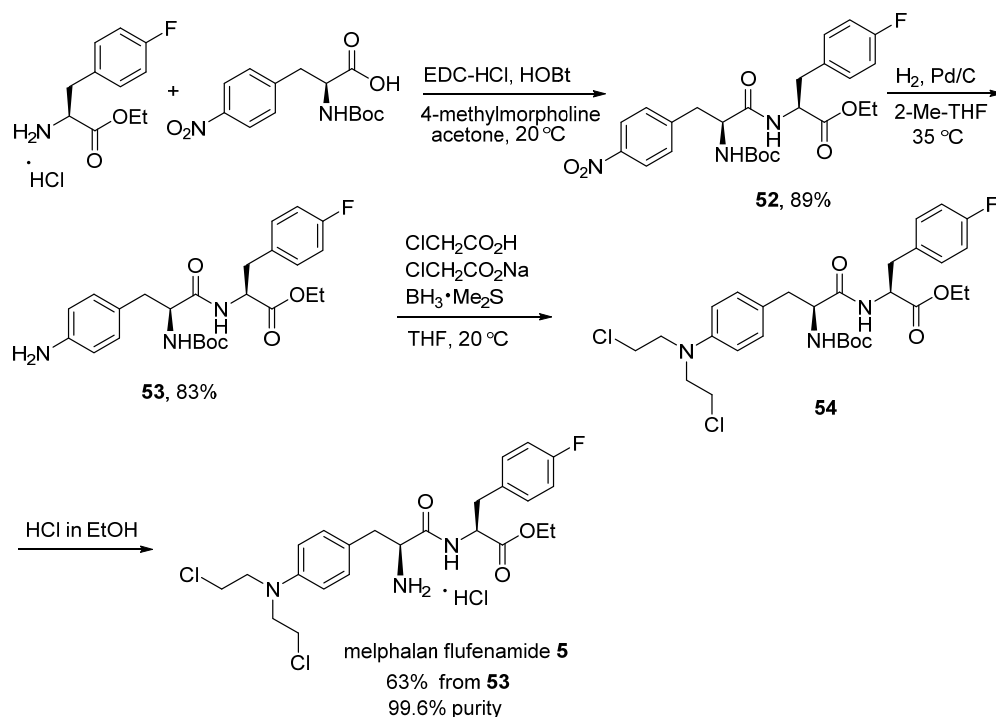


Figure 6. Structures of melphalan flufenamide **5**, its metabolites and analogs.

A four-step process suitable for commercial production of melphalan flufenamide **5** (Scheme 5) starts from the coupling of 4-fluoro-*L*-phenylalanine [58] ethyl ester with Boc-4-nitro-*L*-phenylalanine providing dipeptide **52** in excellent yield (89%) and purity (99.9%) [59,60]. Reduction of the nitro group of **52** with Pd/C as a catalyst in 2-methyltetrahydrofuran afforded **53** in high yield (83%). Next, one step reductive bis-alkylation of amine **53** was achieved using chloroacetic acid, sodium chloroacetate, and the borane-dimethyl sulfide complex as the reducing agent to give *N,N*-bis-chloroethylamino derivative **54**. The use of an excess of sodium chloroacetate in the bis-alkylation reaction minimizes side reactions providing a high purity product (99.6%). Thus, *N,N*-bis-chloroethylamine functionality can be introduced at the late stage of this process. The deprotection of the *N*-Boc group by treatment of HCl in ethanol at room temperature produced melphalan flufenamide **5** hydrochloride in high purity (99.6%). The overall yield of this four-step process was 47%.



Scheme 5. Synthesis of melphalan flufenamide **5**.

7. Cabotegravir (Cabenuva™)

Cabotegravir **6** is developed by ViiV Healthcare as an integrase strand transfer inhibitor (INSTI) of the carbamoyl pyridone type. In the HIV replication cycle, integrase catalyzes the insertion of the viral genome into the genome of host cells. INSTIs prevent the formation of the covalent bond with host DNA by blocking the integrase enzyme, thus inhibiting the incorporation of viral DNA into the host genome [61]. Cabotegravir **6** exhibits slow metabolism, low aqueous solubility, and an extremely long half-life of 21–50 days [62]. Because cabotegravir **6** is metabolized primarily by uridine diphosphate glucuronosyltransferase 1A1, the possibility of interactions with other antiretroviral drugs is minimal [63]. The US FDA approved in 2021 the combination of cabotegravir **6** and non-nucleoside reverse transcriptase inhibitor (NNRTI) rilpivirine as a long-acting injectable regimen for the treatment of HIV-1 in virologically suppressed adults with no suspected resistance to cabotegravir **6** or rilpivirine [64,65].

Integrase inhibitors cabotegravir **6**, dolutegravir **55**, and bictegravir **56** are structurally similar compounds with different chiral oxazine ring sizes (Figure 7). In general, the difluorobenzyl derivative cabotegravir **6** showed an improvement in potency against the Q148K compared to its monofluoro analog **57**. The SAR studies showed the importance of the aromatic fluorine atoms in improving the antiviral activity of cabotegravir **6** by approximately four-fold compared with its monofluoro counterpart **57** [66].

Synthetic route to cabotegravir **6** starts from 4-methoxy β -ketoester **58** (Scheme 6) [67,68]. The reaction of ester **58** with neat *N,N*-dimethylformamide dimethylacetal (DMF-DMA) at room temperature afforded enamine **59**. After removing excess DMF-DMA, the resulting mixture was treated with aminoacetaldehyde dimethyl acetal and MeOH to afford vinylogous amide **60**. Amide **60** underwent cyclization with dimethyl oxalate in the presence of LiOMe to give pyridinone **61**. Selective hydrolysis of the desired ester group of **61** was effectively achieved with LiOH at low temperature affording the carboxylic acid **62** as a white solid in 61% overall yield from **58**. The acetal deprotection using MeSO₃H and HOAc in MeCN gave the aldehyde **63** which was directly subjected to the cyclization with (*S*)-alaninol at 64 °C to form the oxazolidine ring in a 34:1 diastereomeric excess. The diastereoselectivity could be improved to 41:1 after recrystallization from methanol. The reaction of carboxylic acid **64** with

N,N'-carbonyldiimidazole (CDI) followed by 2,4-difluorobenzylamine [68] afforded amide **65** in 95% yield. Demethylation was accomplished by using LiBr as a deprotecting agent in THF/water to give the cabotegravir **6** in a 93% yield.

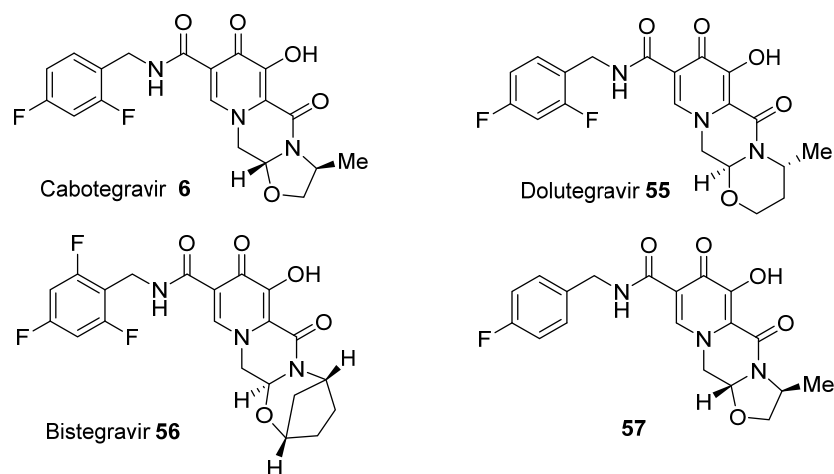
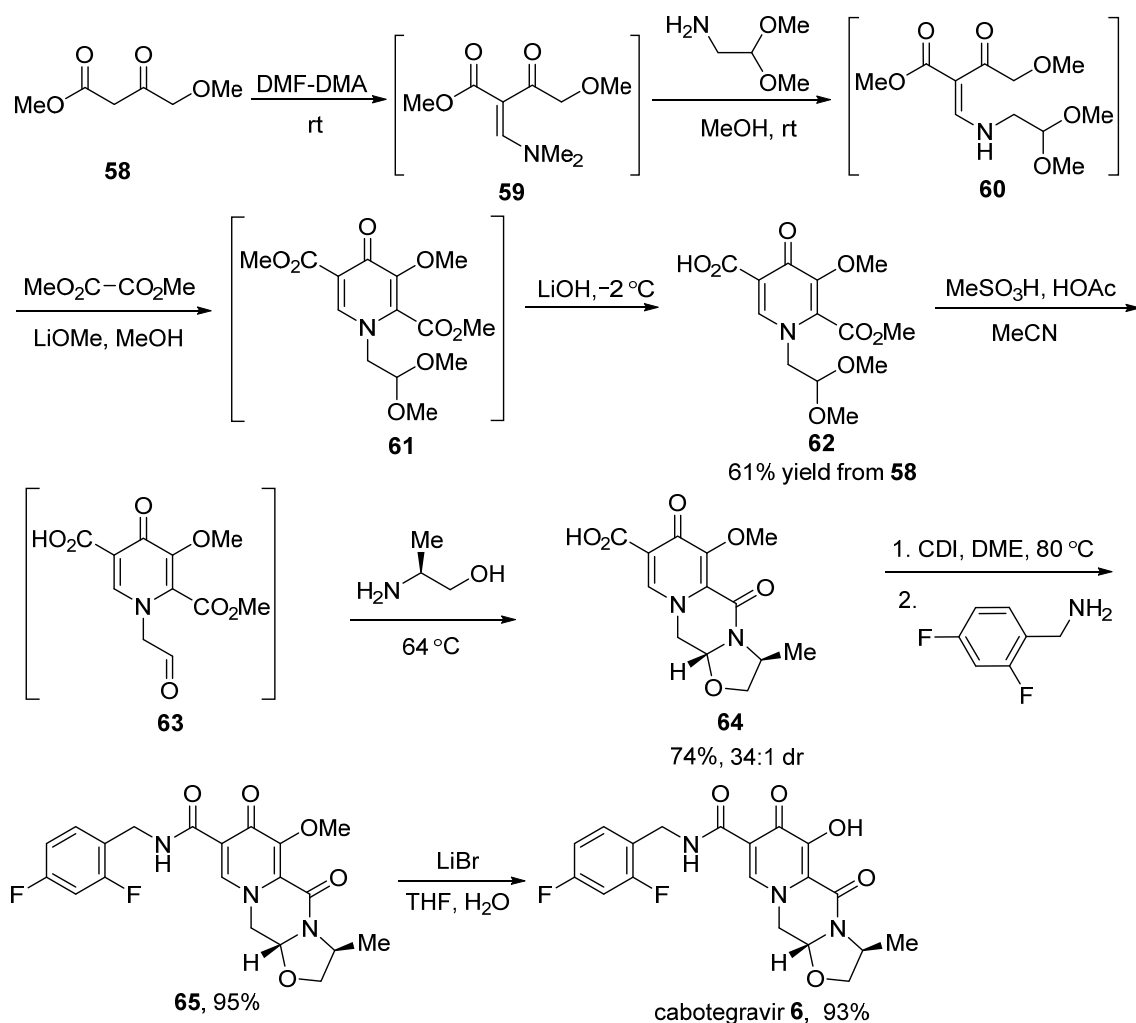
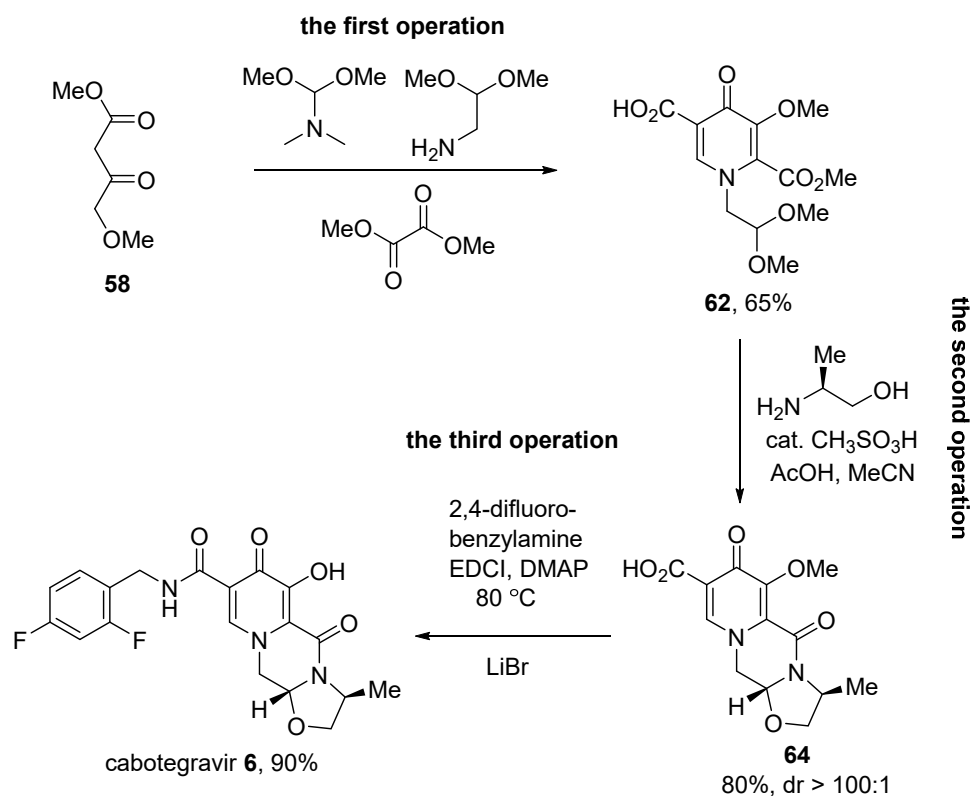


Figure 7. HIV-1 integrase strand transfer inhibitors.



Scheme 6. Synthesis of cabotegravir 6.

Recently, a flow system to realize the seven-step synthesis of cabotegravir **6** was developed (Scheme 7) [69]. The flow system consisted of three distinct flow operations and afforded the desired cabotegravir **6** in a better yield compared to the step-by-step procedure. The advantages of the flow system include low cost, time saving, and universality (can be used to obtain antiretroviral pharmaceuticals dolutegravir **55** and bictegravir **56**). This process is scalable and can be used for industrial production.



Scheme 7. Flow synthesis of the HIV integrase inhibitor cabotegravir **6**.

8. Difelikefalin (Korsuva™)

Difelikefalin **7**, also called CR845, was developed by Cara Therapeutics as an agonist of the kappa opioid receptor (KOR) for treating the disease of pruritus [70,71]. Difelikefalin **7** is a peptide, and the chemical structure is (D-Phe-D-Phe-D-Leu-D-Lys-[ω (4-aminopiperidine-4-carboxylic acid)]-OH), which contains three natural AAs and one unnatural AA. The SAR studies by Cara Therapeutics disclosed that the unnatural amino acid moiety, 4-aminopiperidine-4-carboxylic acid, was crucial for the activity of the kappa opioid agonist. As shown in Figure 8, replacing the 4-aminopiperidine-4-carboxylic acid with proline led to a decrease in KOR activity, as the KOR EC₅₀ value for difelikefalin was 0.048 nM while the value for its analog **66** was 0.075 nM [72]. On the other hand, the other moiety of difelikefalin **7**, the *N*-terminal D-phenylalanine, is also an important pharmacophore for the binding activity of KOR [73]. For example, changing this D-Phe part to another amino acid (**67**) usually led to several folds poorer KOR EC₅₀ values. According to the clinical results, difelikefalin **7** received its first and only therapy from the FDA for treating the disease of pruritus associated with chronic kidney disease (CKD-aP) in adults undergoing hemodialysis in August 2021 [74].

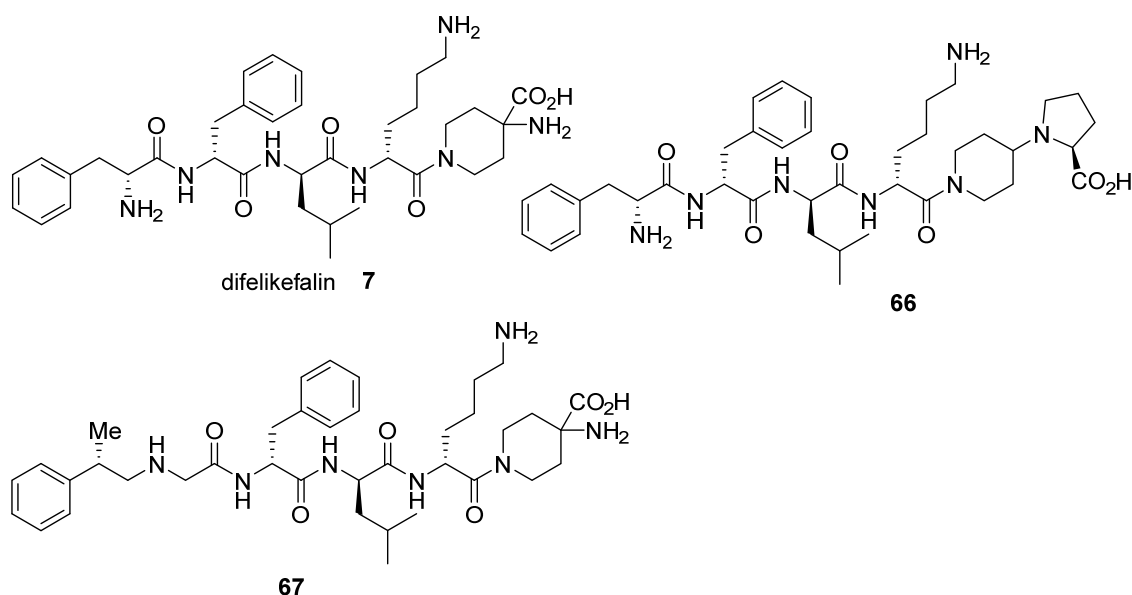
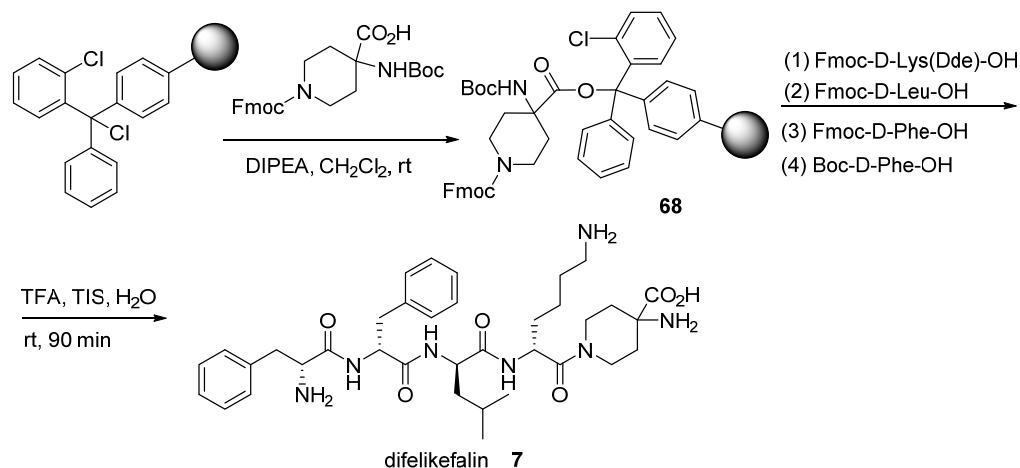


Figure 8. Difelikefalin 7 and its analogs.

Since difelikefalin 7 is a peptide, Cara Therapeutics developed a solid phase peptide synthesis method for its preparation [72]. As presented in Scheme 8, the peptide synthesis started from 2-chlorotrityl chloride resin, which was coupled with *N*-Boc-amino-(4-*N*-Fmoc-piperidiny) carboxylic acid in the presence of DIPEA in dichloromethane at room temperature [75]. The resulting resin **68** was then coupled with Fmoc-D-Lys(Dde)-OH, Fmoc-D-Leu-OH, Fmoc-D-Phe-OH, and Boc-D-Phe-OH, which was followed by the removal of the protecting groups and resin in the presence of TFA and triisopropylsilane (TIS) at room temperature for 90 min. The obtained crude difelikefalin 7 was precipitated from the ether and purified on a HPLC column.



Scheme 8. Synthesis of difelikefalin 7.

9. Odevixibat (Bylvay™)

Odevixibat **8** was developed by Albireo Pharma, Inc. as a potent and selective inhibitor of the ileal bile acid transporter (IBAT) for the treatment of all subtypes of progressive familial intrahepatic cholestasis (PFIC) [76–78]. Odevixibat **8** was demonstrated to be safe and its oral administration was well tolerated [79]. Odevixibat **8** is a chiral compound, which contains one 2-aminobutyric acid and one 4-hydroxyphenylglycine amino acid moieties, and one 2,3,4,5-tetrahydrobenzo[*f*][1,2,5]thiadiazepine 1,1-dioxide heterocyclic unit. The SAR studies by Albireo disclosed that odevixibat **8** exhibits better IBAT inhibitory activity

compared with its analogs. The dipeptide moiety is very important for the activity [80]. For example, the IC_{50} (IBAT) value for odevixibat **8** was 0.16 nmol/L, which was two-fold over its analog **69** (Figure 9) containing an alanine unit instead of a 2-aminobutanoate species ($IC_{50} = 0.3$ nM). Additionally, changing the 4-hydroxyphenylglycine AA moiety to phenylglycine (**70**) led to slightly decreased activity, i.e., an IC_{50} value of 0.18 nM. In particular, if both of the two AAs of odevixibat **8** were changed into others (**71**), a dramatically lower activity was observed with an IC_{50} value of 1.2 nM (about eight-fold). Odevixibat **8** obtained its first approval from the EU and FDA in July 2021 for the treatment of PFIC with more than six-month of age in the EU and the treatment of pruritus in all subtypes of PFIC in the USA [81].

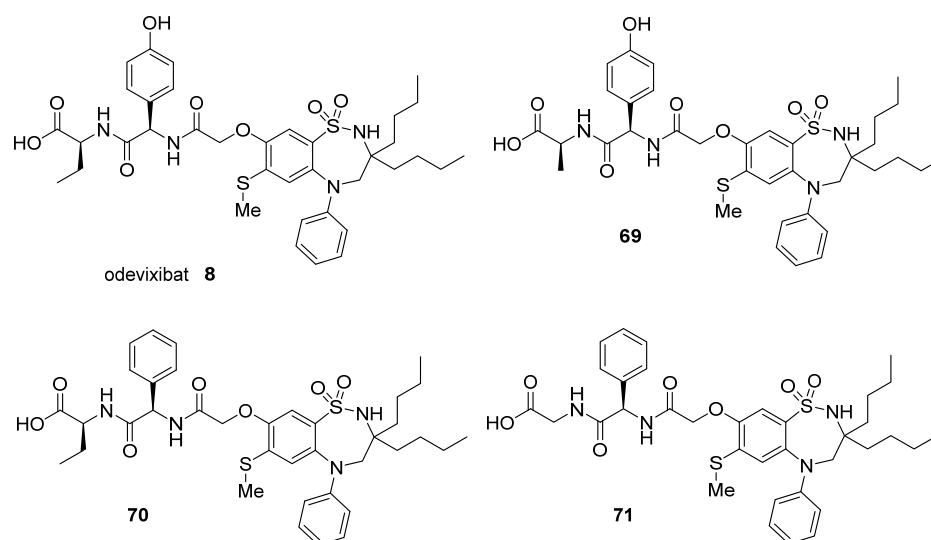
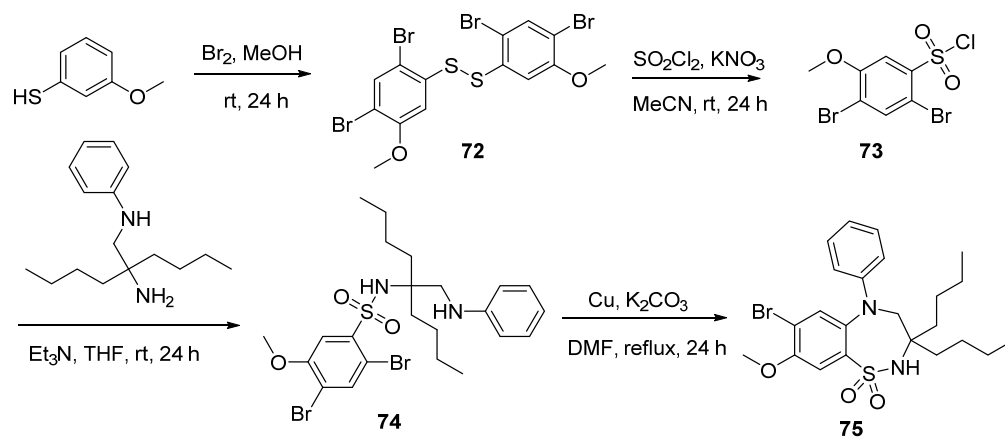


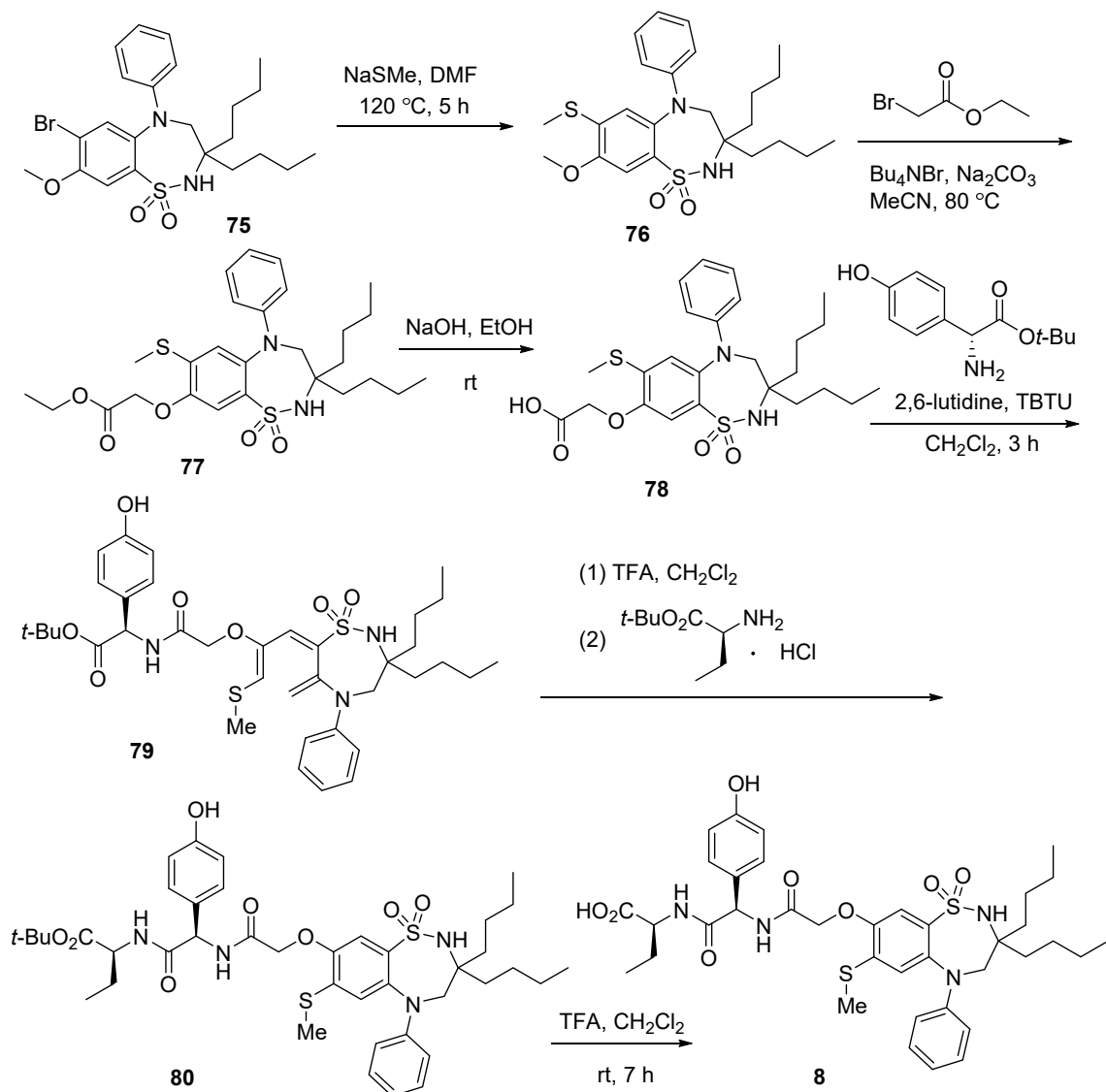
Figure 9. Structures of odevixibat **8** and analogs.

Astrazeneca patented a synthetic method for the preparation of odevixibat **8**, which employed poly-substituted 2,3,4,5-tetrahydrobenzo[*f*][1,2,5]thiadiazepine 1,1-dioxide **75** as the key intermediate [82]. The synthesis of intermediate **75** was presented in Scheme 9 with 3-methoxybenzenethiol as the starting material [83]. Treatment of 3-methoxybenzenethiol with bromine in methanol at room temperature for 24 h afforded 1,2-bis(2,4-dibromo-5-methoxyphenyl)disulfide (**72**), which was converted into sulfonyl chloride **73** via the reaction with sulfonyl chloride in the presence of potassium nitrate in acetonitrile. Then, the reaction of sulfonyl chloride **73** with 2-butyl-*N*¹-phenylhexane-1,2-diamine at room temperature generated the sulfonamide intermediate **74** with triethylamine as a base. Finally, the Cu-promoted intramolecular cyclization reaction of sulfonamide **74** under reflux in DMF for 24 h provided the key 2,3,4,5-tetrahydrobenzo[*f*][1,2,5]thiadiazepine 1,1-dioxide intermediate **75**.

After the key heterocyclic moiety was constructed, the bromo group on the phenyl ring of the intermediate **75** was substituted with methylthio group via reaction with NaSMe in DMF at 120 °C for 5 h, generating the intermediate **76** (Scheme 10) [82]. Subsequently, the intermediate **76** was subjected to the reaction with ethyl 2-bromoacetate and sodium carbonate in the presence of Bu₄NBr yielding the ester **77**. Hydrolysis of ester **77** with the use of sodium hydroxide provided the acid **78**, which underwent the condensation reaction with *tert*-butyl (*R*)-2-amino-2-(4-hydroxyphenyl)acetate in the presence of *O*-(benzotriazol-1-yl)-*N,N,N',N'*-tetramethyluronium tetrafluoroborate (TBTU) and 2,6-lutidine in dichloromethane. The generated *tert*-butyl ester **79** was treated by TFA in dichloromethane followed by the second peptide condensation reaction with *tert*-butyl (*S*)-2-aminobutanoate, providing the dipeptide **80**. Finally, the target odevixibat **8** was obtained via the hydrolysis of the intermediate **80** under acidic conditions.



Scheme 9. Synthesis of the intermediate 75.



Scheme 10. Synthesis of odevixibat 8.

10. Ibrexafungerp (Brexafemme™)

Ibrexafungerp **9**, with the trade name Brexafemme™, was approved in June of 2021 by the FDA for the treatment of vulvovaginal candidiasis (VVC). As a derivative of the natural product enfumafungin, it was developed by the company Scynexis [84]. Ibrexafungerp is a triterpenoid antifungal drug for adult and post-menarchal pediatric females with VVC. Although the specific binding site of ibrexafungerp is not clear, it could blockade the biosynthesis of β -1,3-glucan, a crucial component of the fungal cell wall [85]. Ibrexafungerp **9** is a chiral compound derived from the natural product enfumafungin containing a pyridyl triazole moiety and an aminoether moiety, which are suggested to be quite important for the drug efficiency. For example, the IC_{50} of ibrexafungerp for β -1,3-glucan synthase inhibition in *Candida albicans* (MY 1055) microsomal membrane fragments is $0.001 \mu\text{g/mL}$. When the pyridyl group on triazole unit is replaced by hydrogen, **81** (Figure 10) demonstrates a raised IC_{50} value of $0.007 \mu\text{g/mL}$. Additionally, when the substituents on the aminoether units change slightly, the IC_{50} values of **82** and **83** are 0.002 and $0.007 \mu\text{g/mL}$, respectively [86]. Actually, ibrexafungerp **9** ($ED_{99} = 0.84 \text{ mpk}$ vs. *C. albicans*) was developed via SAR optimization by the Scynexis Inc. of the substituent on triazole moiety from their previously reported β -1,3-glucan synthesis inhibitor, MK-5204 ($ED_{99} = 6.4 \text{ mpk}$ vs. *C. albicans*) [86]. Ibrexafungerp is supplied as tablets for oral administration. It should be mentioned that this non-azole antifungal drug is not suitable for pregnant patients based on animal toxicity studies [84].

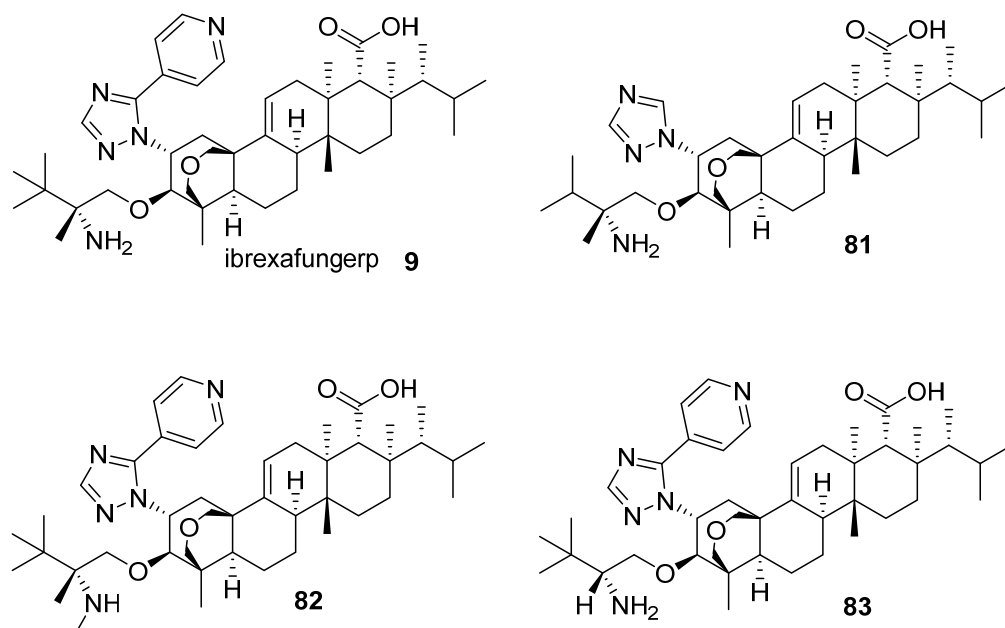
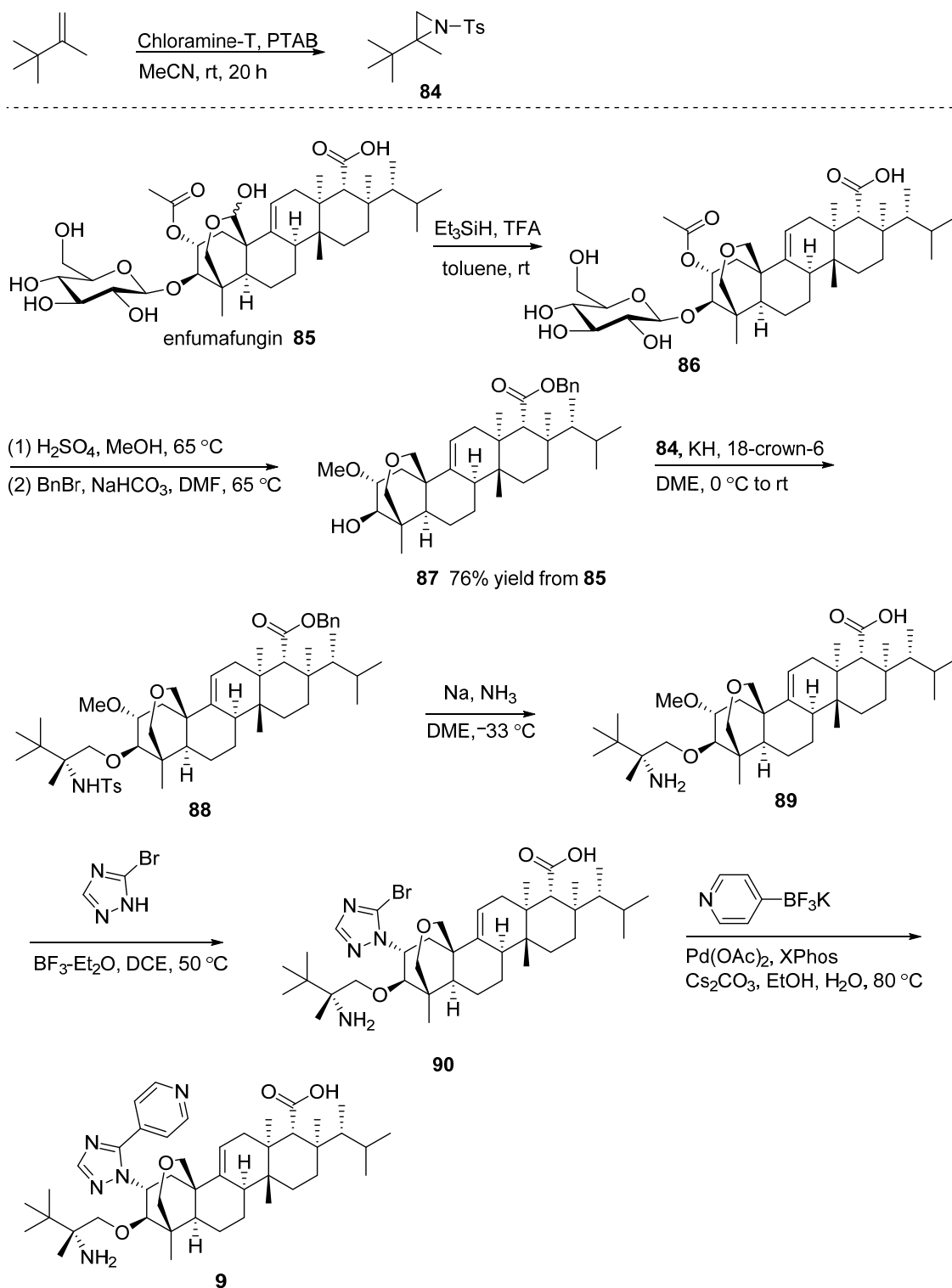


Figure 10. Structures of ibrexafungerp **9** and analogs.

The synthetic method for the preparation of ibrexafungerp **9** by Merck and Scynexis Inc. is presented in Scheme 11, which used a natural product, enfumafungin (**85**) as the starting material [86]. First, aziridination of 2,3,3-trimethylbut-1-ene with the use of chloramine-T and phenyltrimethylammonium tribromide (PTAB) in acetonitrile at room temperature provided the aziridine intermediate **84** [87]. On the other hand, the reduction of the bridging hemiacetal of enfumafungin (**85**) by triethylsilane in the presence of TFA afforded the deoxyenfumafungin intermediate **86**. Then, the removal of the glycoside by sulfuric acid in methanol and the replacement of the acetoxy group by methyl ether followed by the esterification of the carboxylic acid group via treatment with benzyl bromide and sodium bicarbonate afforded the intermediate **87** [87]. Subsequently, intermediate **87** was subjected to an alkylation reaction with aziridine intermediate **84** in the presence of KH and 18-crown-6 resulting in the amine **88**, which then underwent a Birch reduction reaction

to remove the tosyl and benzyl protecting groups. The obtained free aminoether **89** was treated with 3-bromo-1,2,4-triazole in the presence of borontrifluoride diethyletherate in dichloroethane providing the intermediate **90** [88]. Finally, the Suzuki coupling reaction between the intermediate **90** and potassium pyridine-4-trifluoroborate gave the targeted ibrexafungerp **9**.

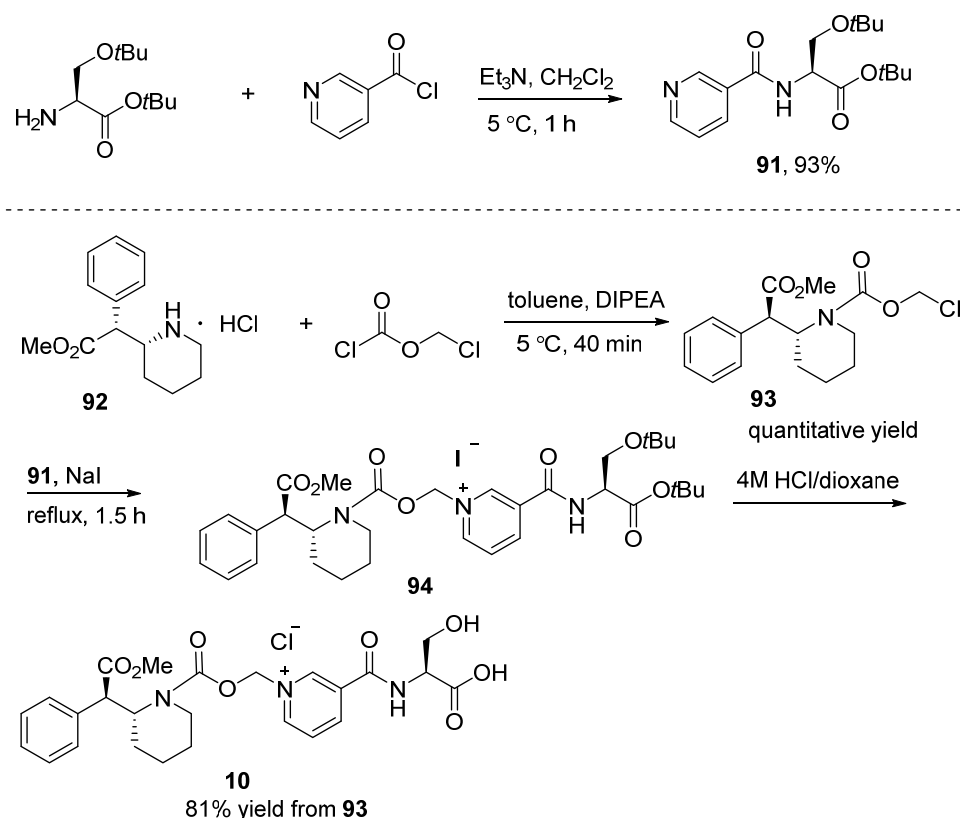


Scheme 11. Synthesis of ibrexafungerp **9**.

11. Serdexmethylphenidate and Dexmethylphenidate (Azstarys™)

Serdexmethylphenidate **10** is a prodrug of d-methylphenidate, which is an ammonium salt containing two AA moieties. As shown in Figure 1, the two AAs, methyl (*R*)-2-phenyl-2-((*R*)-piperidin-2-yl)acetate and L-serine were linked by nicotinoyl and carbamate. Serdexmethylphenidate and d-methylphenidate capsule (SDX/d-MPH) has been developed as a new stimulant and used in children with attention deficit hyperactivity disorder (ADHD). The randomized, double-blind, dose-optimized studies showed that a significant treatment effect for SDX/d-MPH compared with placebo was observed from 1 to 10 h postdose [89–91]. In March 2021, SDX/d-MPH developed by Corium was approved by the FDA with the trade name Azstarys™ for attention deficit hyperactivity disorder (ADHD) in patients 6 years of age and older.

Kempharm, INC. patented a method for the preparation of serdexmethylphenidate **10** in 2018, which used *tert*-butyl *O*-(*tert*-butyl)-L-serinate (H-Ser(*t*Bu)-*O**t*Bu) as the starting material (Scheme 12) [92]. First, the addition of nicotinoyl chloride into the solution of H-Ser(*t*Bu)-*O**t*Bu in dichloromethane in the presence of triethylamine at 5 °C afforded the nicotinoyl-Ser(*t*Bu)-*O**t*Bu **91** in 93% yield after 1 h. On the other hand, the reaction of methyl (*R*)-2-phenyl-2-((*R*)-piperidin-2-yl)acetate hydrochloride [93] (**92**) with chloromethyl chloroformate using DIPEA as a base generated the amide **93** in quantitative yield, which then was refluxed with nicotinoyl-Ser(*t*Bu)-*O**t*Bu **91** and NaI in acetone resulting in the iodide salt intermediate **94**. Finally, the iodide salt intermediate **94** was treated with 4M HCl in dioxane, affording the target serdexmethylphenidate **10**. It should be mentioned that an anion exchange resin, Dowex 1*8 chloride was used to replace the anionic counter iodide ion with the chloride ion in the last step.



Scheme 12. Synthesis of serdexmethylphenidate **10**.

12. Pafolacianine (Cytalux™)

Pafolacianine **11**, also named OTL38, was a tumor-targeted near-infrared fluorescent dye, which provides visual evidence of its remarkable cancer-illuminating capabilities. It was developed by On Target Laboratories as an adjunct to visual inspection and palpation

by providing intra-operative imaging of folate receptor positive (FR+) ovarian cancer according to its fundamental properties [94]. Pafolacianine **11** contains a pteroyl amide unit, a tyrosine AA moiety and a S0456 fluorescent species. The evaluation of the binding affinity was performed, and the results disclose that L-tyrosine is important for the binding affinity. The relative affinity (RA) value calculated for folic acid **95** (Figure 11) and pafolacianine **11**, was 1.0 and 0.8, respectively. However, when changing the L-tyrosine into D-tyrosine, the RA value for compound **96** will be 0.09 [95]. Based on the safety and efficacy results of phase III [96], pafolacianine sodium injection obtained its approval from the FDA in November 2021 with the trade name Cytalux™ for use to help identify ovarian cancer lesions [97,98].

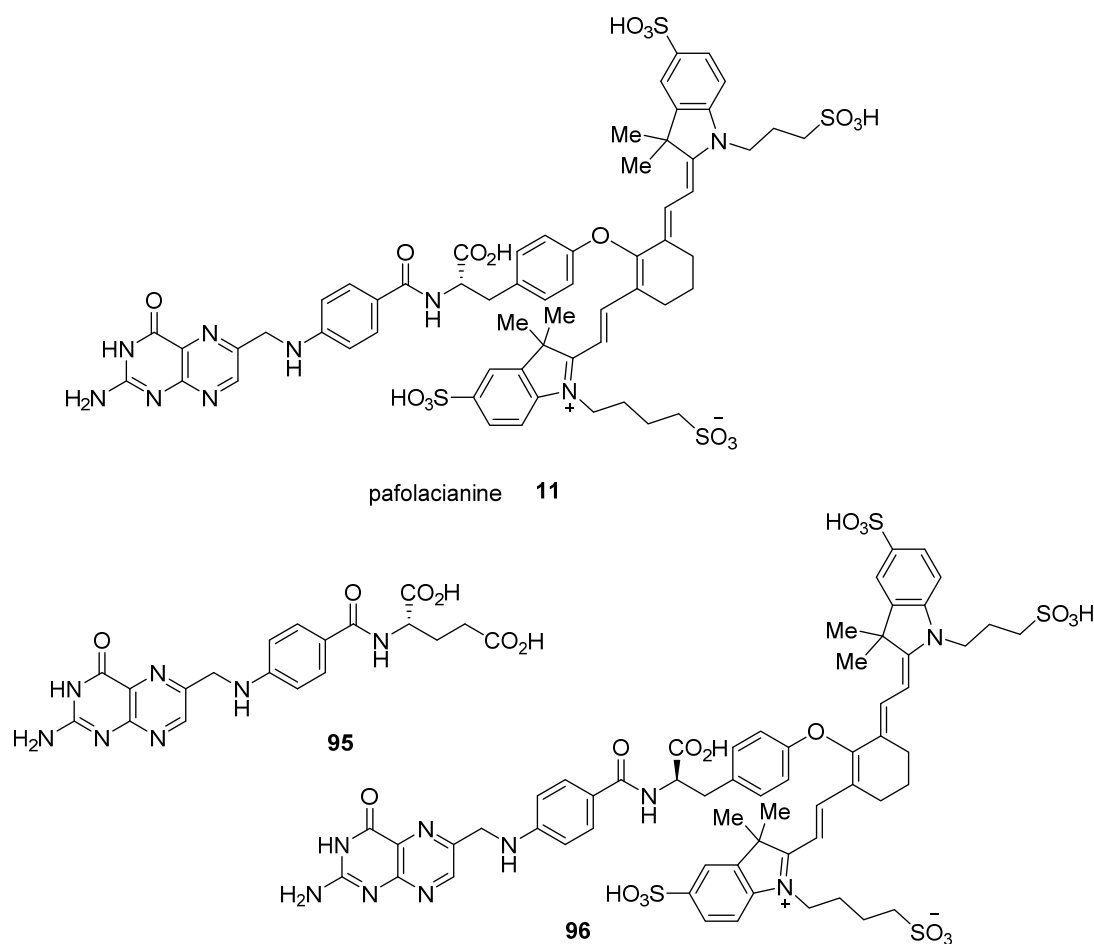
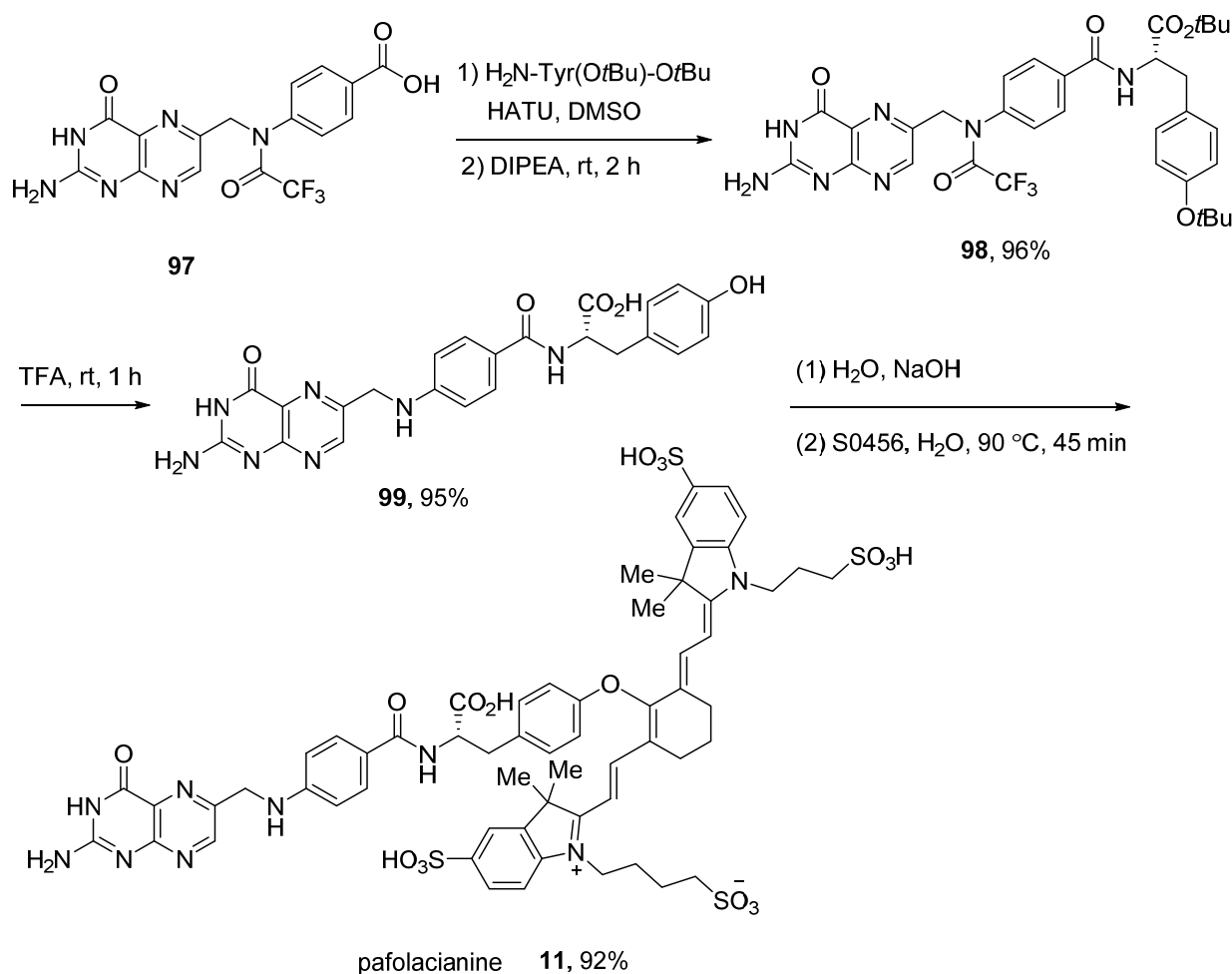


Figure 11. Pafolacianine **11** and its analogs.

The synthesis of pafolacianine **11** is shown in Scheme 13, which used commercially available N¹⁰-trifluoroacetylpteroic acid **97** as the starting material [94,95]. First, condensation of **97** with NH₂-L-Tyr(OtBu)-OtBu with the use of 2-(7-azabenzotriazol-1-yl)-N,N,N',N'-tetramethyluronium hexafluorophosphate (HATU) as the condensing reagent in the presence of DIPEA afforded the corresponding pteroyl-N¹⁰(TFA)-Tyr(OtBu)-OtBu intermediate **98** in 96% yield at room temperature after 2 h. Then, the removal of the *tert*-butyl protecting groups via treatment with TFA at room temperature generated the pteroyl-N¹⁰(TFA)-Tyr(OH)-CO₂H intermediate **99** in 95% yield. Subsequently, the intermediate **99** was treated with aqueous NaOH solution and then reacted with S0456 at 90 °C for 45 min providing the target pafolacianine **11** in 92% yield.



Scheme 13. Synthesis of pafolacianine **11**.

13. Conclusions

The growing acceptance of peptides (biopharmaceuticals) and peptidomimetics (small-molecule pharmaceuticals) as drugs clearly indicates that AA derivatives will remain the preferred structural platform in the development of modern pharmaceuticals. Some of the problematic issues associated with AAs application include racemization, proteolytic and microsomal metabolism, clearance rates, and the membrane permeability of AA-derived compounds. These issues can be addressed by the strategic substitution of fluorine for hydrogen and the incorporation of trifluoromethyl and chlorodifluoromethyl groups. Steric, electronic and physical properties of the fluorinated groups [99–102] can be rationally applied to enhance configurational stability, reduce proteolytic and microsomal degradation, slow down clearance rates and enhance membrane permeability [103–107], allowing to ameliorate the inherent problems associated with AA-derivatives. Of special note is that promiscuity and off-target toxicity of drug candidates are shown to be reduced by the introduction of elements of chirality, in particular, stereogenic centers. Quite unsurprisingly, all 11 drugs reviewed in this work are chiral, containing at least one and up to 12 stereogenic carbons. In this regard, it should be emphasized that the reported stereochemical outcome of the enantioselective reactions discussed in this review is missing the issue of the SDE properties [108,109] of enantiomerically enriched intermediates and final products. It has been unambiguously demonstrated that fluorine [110–112], chiral amines [113,114], α - [115,116], and β -amino acids [117] are SDE-phoric groups, showing a significant magnitude of SDE under a variety of physicochemical transformations. As a result of the SDE ignorance, the reported data of stereochemical outcome can be collected with substantial

mistakes leading to an erroneous presentation of the synthetic value and mechanistic interpretation of the corresponding reactions [118,119]. Studying the SDE properties of chiral molecules is an important issue in laboratory practice and drug development, reflecting the current standards in the administration of chiral drugs as pure enantiomers [120–122].

Author Contributions: Conceptualization, J.H., V.A.S. and A.S.; validation, Q.W., J.H., A.L. and A.S.; writing—original draft preparation, Q.W., J.H., A.L., V.A.S. and A.S.; writing—review and editing, J.H., V.A.S., G.B. and A.S.; supervision, J.H., V.A.S. and A.S. All authors have read and agreed to the published version of the manuscript.

Funding: This work was funded by the National Natural Science Foundation of China (No. 21761132021), and IKERBASQUE, Basque Foundation for Science. The financial support from the University of the Basque Country UPV/EHU (UFIQOSYC11/22), Basque Government (GVgrant IT1236-19), and Ministerio de Ciencia e Innovación (grant PID2019-109633GBC21) for A. L. are also acknowledged.

Institutional Review Board Statement: Not applicable.

Informed Consent Statement: Not applicable.

Data Availability Statement: Not applicable.

Conflicts of Interest: The authors declare no conflict of interest.

References

1. Liu, A.; Han, J.; Nakano, A.; Konno, H.; Moriwaki, H.; Abe, H.; Izawa, K.; Soloshonok, V.A. New pharmaceuticals approved by FDA in 2020: Small-molecule drugs derived from amino acids and related compounds. *Chirality* **2022**, *34*, 86–103. [[CrossRef](#)]
2. Han, J.; Lyutenko, N.V.; Sorochinsky, A.E.; Okawara, A.; Konno, H.; White, S.; Soloshonok, V.A. Tailor-made amino acids in pharmaceutical industry: Synthetic approaches to aza-tryptophan derivatives. *Chem. Eur. J.* **2021**, *27*, 17510–17528. [[CrossRef](#)] [[PubMed](#)]
3. Han, J.; Konno, H.; Sato, T.; Izawa, K.; Soloshonok, V.A. Peptidomimetics and peptide-based blockbuster drugs. *Curr. Org. Chem.* **2021**, *25*, 1627–1658. [[CrossRef](#)]
4. Han, J.; Konno, H.; Sato, T.; Soloshonok, V.A.; Izawa, K. Tailor-made amino acids in the design of small-molecule blockbuster drugs. *Eur. J. Med. Chem.* **2021**, *220*, 113448. [[CrossRef](#)]
5. Yin, Z.; Hu, W.; Zhang, W.; Konno, H.; Moriwaki, H.; Izawa, K.; Han, J.; Soloshonok, V.A. Tailor-made amino acid-derived pharmaceuticals approved by the FDA in 2019. *Amino Acids* **2020**, *52*, 1227–1261. [[CrossRef](#)] [[PubMed](#)]
6. Liu, J.; Han, J.; Izawa, K.; Sato, T.; White, S.; Meanwell, N.A.; Soloshonok, V.A. Cyclic tailor-made amino acids in the design of modern pharmaceuticals. *Eur. J. Med. Chem.* **2020**, *208*, 112736. [[CrossRef](#)] [[PubMed](#)]
7. Soloshonok, V.A.; Izawa, K. (Eds.) *Asymmetric Synthesis and Application of α -Amino Acids*; ACS Symposium Series #1009; Oxford University Press: Washington, DC, USA, 2009.
8. Blaskovich, M.A.T. Unusual amino acids in medicinal chemistry. *J. Med. Chem.* **2016**, *59*, 10807–10836. [[CrossRef](#)] [[PubMed](#)]
9. Henninot, A.; Collins, J.C.; Nuss, J.M. The current state of peptide drug discovery: Back to the future? *J. Med. Chem.* **2018**, *61*, 1382–1414. [[CrossRef](#)] [[PubMed](#)]
10. Hodgson, D.R.W.; Sanderson, J.M. The synthesis of peptides and proteins containing non-natural amino acids. *Chem. Soc. Rev.* **2004**, *33*, 422–430. [[CrossRef](#)] [[PubMed](#)]
11. Wang, S.; Wang, Y.; Wang, J.; Sato, T.; Izawa, K.; Soloshonok, V.A.; Liu, H. The second-generation of highly potent hepatitis C virus (HCV) NS3/4A protease inhibitors: Evolutionary design based on tailor-made amino acids, synthesis and major features of bioactivity. *Curr. Pharm. Des.* **2017**, *23*, 4493–4554. [[CrossRef](#)] [[PubMed](#)]
12. Sato, T.; Izawa, K.; Aceña, J.L.; Liu, H.; Soloshonok, V.A. Tailor-made α -amino acids in the pharmaceutical industry: Synthetic approaches to (1R, 2S)-1-amino-2-vinylcyclopropane-1-carboxylic acid (vinyl-ACCA). *Eur. J. Org. Chem.* **2016**, *2016*, 2757–2774. [[CrossRef](#)]
13. Liu, J.; Lin, W.; Sorochinsky, A.E.; Butler, G.; Landa, A.; Han, J.; Soloshonok, V.A. Successful trifluoromethoxy-containing pharmaceuticals and agrochemicals. *J. Fluor. Chem.* **2022**, 257–258, 109978. [[CrossRef](#)]
14. Han, J.; Remete, A.M.; Dobson, L.S.; Kiss, L.; Izawa, K.; Moriwaki, H.; Soloshonok, V.A.; O'Hagan, D. Next generation organofluorine containing blockbuster drugs. *J. Fluor. Chem.* **2020**, *239*, 109639. [[CrossRef](#)]
15. Mei, H.; Han, J.; White, S.; Graham, D.J.; Izawa, K.; Sato, T.; Fustero, S.; Meanwell, N.A.; Soloshonok, V.A. Tailor-made amino acids and fluorinated motifs as prominent traits in the modern pharmaceuticals. *Chem. Eur. J.* **2020**, *26*, 11349–11390. [[CrossRef](#)]
16. Mei, H.; Han, J.; Klika, K.D.; Izawa, K.; Sato, T.; Meanwell, N.A.; Soloshonok, V.A. Applications of fluorine-containing amino acids for drug design. *Eur. J. Med. Chem.* **2020**, *186*, 111826. [[CrossRef](#)]
17. Han, J.; Kiss, L.; Mei, H.; Remete, A.M.; Ponikvar-Svet, M.; Sedgwick, D.M.; Roman, R.; Fustero, S.; Moriwaki, H.; Soloshonok, V.A. Chemical aspects of human and environmental overload with fluorine. *Chem. Rev.* **2021**, *121*, 4678–4742. [[CrossRef](#)]

18. Mei, H.; Remete, A.M.; Zou, Y.; Moriwaki, H.; Fustero, S.; Kiss, L.; Soloshonok, V.A.; Han, J. Fluorine-containing drugs approved by the FDA in 2019. *Chin. Chem. Lett.* **2020**, *31*, 2401–2413. [[CrossRef](#)]
19. Yu, Y.; Liu, A.; Dhawan, G.; Mei, H.; Zhang, W.; Izawa, K.; Soloshonok, V.A.; Han, J. Fluorine-containing pharmaceuticals approved by the FDA in 2020: Synthesis and biological activity. *Chin. Chem. Lett.* **2021**, *32*, 3342–3354. [[CrossRef](#)]
20. Wang, J.; Sánchez-Roselló, M.; Aceña, J.L.; del Pozo, C.; Sorochinsky, A.E.; Fustero, S.; Soloshonok, V.A.; Liu, H. Fluorine in pharmaceutical industry: Fluorine-containing drugs introduced to the market in the last decade (2001–2011). *Chem. Rev.* **2014**, *114*, 2432–2506. [[CrossRef](#)]
21. Zhou, Y.; Wang, J.; Gu, Z.; Wang, S.; Zhu, W.; Aceña, J.L.; Soloshonok, V.A.; Izawa, K.; Liu, H. Next generation of fluorine-containing pharmaceuticals, compounds currently in phase II–III clinical trials of major pharmaceutical companies: New structural trends and therapeutic areas. *Chem. Rev.* **2016**, *116*, 422–518. [[CrossRef](#)]
22. Réa, D.; Hughes, T.P. Development of asciminib, a novel allosteric inhibitor of BCR-ABL1. *Crit. Rev. Oncol. Hemat.* **2022**, *171*, 103580. [[CrossRef](#)] [[PubMed](#)]
23. Manley, P.W.; Barys, L.; Cowan-Jacob, S.W. The specificity of asciminib, a potential treatment for chronic myeloid leukemia, as a myristate-pocket binding ABL inhibitor and analysis of its interactions with mutant forms of BCR-ABL1 kinase. *Leuk. Res.* **2020**, *98*, 106458. [[CrossRef](#)]
24. Deeks, E.D. Asciminib: First approval. *Drugs* **2022**, *82*, 219–226. [[CrossRef](#)]
25. Wylie, A.A.; Schoepfer, J.; Jahnke, W.; Cowan-Jacob, S.W.; Loo, A.; Furet, P.; Marzinzik, A.L.; Pelle, X.; Donovan, J.; Zhu, W.; et al. The allosteric inhibitor ABL001 enables dual targeting of BCR-ABL1. *Nature* **2017**, *543*, 733–737. [[CrossRef](#)] [[PubMed](#)]
26. Hughes, T.P.; Mauro, M.J.; Cortes, J.E.; Minami, H.; Rea, D.; DeAngelo, D.J.; Breccia, M.; Goh, Y.T.; Talpaz, M.; Hochhaus, A.; et al. Asciminib in chronic myeloid leukemia after ABL kinase inhibitor failure. *N. Engl. J. Med.* **2019**, *381*, 2315–2326. [[CrossRef](#)] [[PubMed](#)]
27. Wang, Q.; Zhang, X.; Sorochinsky, A.E.; Butler, G.; Han, J.; Soloshonok, V.A. Advances in the development of trifluoromethoxylation reagents. *Symmetry* **2021**, *13*, 2380. [[CrossRef](#)]
28. Schoepfer, J.; Jahnke, W.; Berellini, G.; Buonamici, S.; Cotesta, S.; Cowan-Jacob, S.W.; Dodd, S.; Drueckes, P.; Fabbro, D.; Gabriel, T.; et al. Discovery of asciminib (ABL001), an allosteric inhibitor of the tyrosine kinase activity of BCR-ABL1. *J. Med. Chem.* **2018**, *61*, 8120–8135. [[CrossRef](#)]
29. Fu, L.; Wang, A.; He, B.; Sun, J.; Song, C. Preparation Method for 4-(Chlorodifluoro-Methoxy) Aniline. CN104119238A, 29 October 2014.
30. Lee, A. Avacopan: First approval. *Drugs* **2022**, *82*, 79–85. [[CrossRef](#)]
31. Shagdarsuren, G.; Khaidav, G.; Togtokh, A.; Sonomjants, M.; Shagdarsuren, E. Complement anaphylatoxin C5a, endothelial dysfunction and low-grade inflammation in atherosclerotic vascular diseases. *Cent. Asian J. Med. Sci.* **2018**, *4*, 243–252.
32. Jayne, D.R.W.; Merkel, P.A.; Schall, T.J.; Bekker, P. Avacopan for the treatment of ANCA-associated vasculitis. *N. Engl. J. Med.* **2021**, *384*, 599–609. [[CrossRef](#)]
33. Osmana, M.; Tervaerta, J.W.C.; Pagnoux, C. Avacopan for the treatment of ANCA-associated vasculitis. *Expert Rev. Clin. Immunol.* **2021**, *17*, 717–726. [[CrossRef](#)] [[PubMed](#)]
34. Thorley, J. FDA approves avacopan for ANCA-associated vasculitis. *Lancet Rheumatol.* **2022**, *4*, e21. [[CrossRef](#)]
35. Fan, P.; Greenman, K.L.; Leleti, M.R.; Li, Y.; Powers, J.; Tanaka, H.; Yang, J.; Zeng, Y. C5AR Antagonists. WO 2011163640 A1, 24 June 2011.
36. Fan, F.; Kalisiak, J.; Krasinski, A.; LUI, R.; Powers, J.; Punna, S.; Tanaka, H.; Zhang, P. Processes and Intermediates in the Preparation of C5AR Antagonists. U.S. Patent 9745268 B2, 29 August 2017.
37. Han, J.; Takeda, R.; Sato, T.; Moriwaki, H.; Abe, H.; Izawa, K.; Soloshonok, V.A. Optical resolution of rimantadine. *Molecules* **2019**, *24*, 1828. [[CrossRef](#)] [[PubMed](#)]
38. Takeda, R.; Kawamura, A.; Kawashima, A.; Sato, T.; Moriwaki, H.; Izawa, K.; Abe, H.; Soloshonok, V.A. Second-order asymmetric transformation and its application for the practical synthesis of α -amino acids. *Org. Biomol. Chem.* **2018**, *16*, 4968–4972. [[CrossRef](#)] [[PubMed](#)]
39. Moreno-Ajona, D.; Pérez-Rodríguez, A.; Goadsby, P.J. Small-molecule CGRP receptor antagonists: A new approach to the acute and preventive treatment of migraine. *Med. Drug Discov.* **2020**, *7*, 100053. [[CrossRef](#)]
40. Wattiez, A.S.; Sowers, L.P.; Russo, A.F. Calcitonin gene-related peptide (CGRP): Role in migraine pathophysiology and therapeutic targeting. *Expert Opin. Ther. Targets* **2020**, *24*, 91–100. [[CrossRef](#)]
41. Edvinsson, L. The CGRP pathway in migraine as a viable target for therapies. *Headache* **2018**, *58*, 33–47. [[CrossRef](#)]
42. Dubowchik, G.M.; Conway, C.M.; Xin, A.W. Blocking the CGRP pathway for acute and preventive treatment of migraine: The evolution of success. *J. Med. Chem.* **2020**, *63*, 6600–6623. [[CrossRef](#)]
43. Deeks, E.D. Atogepant: First approval. *Drugs* **2022**, *82*, 65–70. [[CrossRef](#)]
44. Chen, F.; Molinaro, C.; Wuelfing, W.P.; Yasuda, N.; Hong, Y.L.; Lynch, J.; Andreani, T. Process for Making CGRP Receptor Antagonists. WO2013169348, 13 May 2013.
45. Bell, I.M.; Fraley, M.E.; Gallicchio, S.N.; Ginnetti, A.; Mitchell, H.J.; Paone, D.V.; Staas, D.D.; Wang, G.; Zartman, C.B.; Stevenson, H.E. Piperidinone Carboxamide Azaindane CGRP Receptor Antagonists. WO2012064910A1, 18 May 2012.
46. Takeda, R.; Kawamura, A.; Kawashima, A.; Sato, T.; Moriwaki, H.; Izawa, K.; Akaji, K.; Wang, S.; Liu, H.; Aceña, J.L.; et al. Chemical dynamic kinetic resolution and (S)/(R)-interconversion of unprotected α -amino acids. *Angew. Chem. Int. Ed.* **2014**, *53*, 12214–12217. [[CrossRef](#)]

47. Zhou, S.; Wang, J.; Chen, X.; Aceña, J.L.; Soloshonok, V.A.; Liu, H. Chemical kinetic resolution of unprotected β -substituted- β -amino acids using recyclable chiral ligands. *Angew. Chem. Int. Ed.* **2014**, *53*, 7883–7886. [[CrossRef](#)] [[PubMed](#)]
48. Canon, J.; Rex, K.; Saiki, A.Y.; Mohr, C.; Cooke, K.; Bagal, D.; Gaida, K.; Holt, T.; Knutson, C.G.; Koppada, N.; et al. The clinical KRAS(G12C) inhibitor AMG 510 drives anti-tumour immunity. *Nature* **2019**, *575*, 217–223. [[CrossRef](#)] [[PubMed](#)]
49. Hobbs, G.A.; Der, C.J.; Rossman, K.L. RAS isoforms and mutations in cancer at a glance. *J. Cell Sci.* **2016**, *129*, 1287–1292. [[CrossRef](#)] [[PubMed](#)]
50. Lanman, B.A.; Allen, J.R.; Allen, J.G.; Amegadzie, A.K.; Ashton, K.S.; Booker, S.K.; Chen, J.J.; Chen, N.; Frohn, M.J.; Goodman, G.; et al. Discovery of a covalent Inhibitor of KRAS^{G12C} (AMG 510) for the treatment of solid tumors. *J. Med. Chem.* **2020**, *63*, 52–65. [[CrossRef](#)]
51. Blair, H.A. Sotorasib: First approval. *Drugs* **2021**, *81*, 1573–1579. [[CrossRef](#)]
52. Ganguly, A.; Yoo, E. Sotorasib: A KRAS^{G12C} inhibitor for non-small cell lung cancer. *Trends Pharm. Sci.* **2022**, *43*, 536–537. [[CrossRef](#)]
53. Parsons, A.T.; Beaver, M.B. Improved Synthesis of KRAS G12C Inhibitor Compound. WO 2021097212, 20 May 2021.
54. Miettinen, J.J.; Kumari, R.; Traustadottir, G.A.; Huppunen, M.E.; Sergeev, P.; Majumder, M.M.; Schepsky, A.; Gudjonsson, T.; Lievonen, J.; Bazou, D.; et al. Aminopeptidase expression in multiple myeloma associates with disease progression and sensitivity to melflufen. *Cancers* **2021**, *13*, 1527. [[CrossRef](#)]
55. Morabito, F.; Tripepi, G.; Martino, E.A.; Vigna, E.; Mendicino, F.; Morabito, L.; Todoerti, K.; Al-Janazreh, H.; D'Arrigo, G.; Canale, F.A.; et al. Spotlight on melphalan flufenamide: An up-and-coming therapy for the treatment of myeloma. *Drug Des. Devel. Ther.* **2021**, *15*, 2969–2978. [[CrossRef](#)]
56. Gullbo, J.; Tullberg, M.; Våbenø, J.; Ehrsson, H.; Lewensohn, R.; Nygren, P.; Larsson, R.; Luthman, K. Structure–activity relationship for alkylating dipeptide nitrogen mustard derivatives. *Oncol. Res.* **2003**, *14*, 113–132. [[CrossRef](#)]
57. Dhillon, S. Melphalan Flufenamide (Melflufen): First approval. *Drugs* **2021**, *81*, 963–969. [[CrossRef](#)]
58. Wang, Y.; Song, X.; Wang, J.; Moriwaki, H.; Soloshonok, V.A.; Liu, H. Recent approaches for asymmetric synthesis of α -amino acids *via* homologation of Ni(II) complexes. *Amino Acids* **2017**, *49*, 1487–1520. [[CrossRef](#)]
59. Cotton, H.; Bäckström, B.; Fritzson, I.; Lehmann, F.; Monemi, T.; Oltner, V.; Sölver, E.; Wahlström, N.; Wennerber, J. Development of a safe process for manufacturing of the potent anticancer agent melflufen hydrochloride. *Org. Process Res. Dev.* **2019**, *23*, 1191–1196. [[CrossRef](#)]
60. Wahlstrom, N.H.; Wennerberg, J.A. Process for Preparation of Nitrogen Mustard Derivatives. WO2016180740A1, 17 November 2016.
61. Mbhele, N.; Chimukangara, B.; Gordon, M. HIV-1 integrase strand transfer inhibitors: A review of current drugs, recent advances and drug resistance. *Int. J. Antimicrob. Agents* **2021**, *57*, 106343. [[CrossRef](#)] [[PubMed](#)]
62. Zhou, T.; Su, H.; Dash, P.; Lin, Z.; Dyavar Shetty, B.L.; Kocher, T.; Szlachetka, A.; Lamberty, B.; Fox, H.S.; Poluektova, L.; et al. Creation of a nanoformulated cabotegravir prodrug with improved antiretroviral profiles. *Biomaterials* **2018**, *151*, 53–65. [[CrossRef](#)] [[PubMed](#)]
63. Trezza, C.; Ford, S.L.; Spreen, V.; Pan, V.; Piscitelli, S. Formulation and pharmacology of long-acting cabotegravir. *Curr. Opin. HIV AIDS* **2015**, *10*, 239–245. [[CrossRef](#)] [[PubMed](#)]
64. Durham, S.H.; Chahine, E.B. Cabotegravir–rilpivirine: The first complete long-acting injectable regimen for the treatment of HIV-1 infection. *Ann. Pharmacother.* **2021**, *55*, 1397–1409. [[CrossRef](#)] [[PubMed](#)]
65. Voelker, R. Monthly injection is approved for patients with HIV. *JAMA* **2021**, *325*, 816. [[CrossRef](#)] [[PubMed](#)]
66. Johns, B.A.; Kawasuji, T.; Weatherhead, J.G.; Taishi, T.; Temelkoff, D.P.; Yoshida, H.; Akiyama, T.; Taoda, Y.; Murai, H.; Kiyama, R.; et al. Carbamoyl pyridone HIV-1 integrase inhibitors 3. a diastereomeric approach to chiral nonracemic tricyclic ring systems and the discovery of dolutegravir (S/GSK1349572) and (S/GSK1265744). *J. Med. Chem.* **2013**, *60*, 5901–5916. [[CrossRef](#)] [[PubMed](#)]
67. David, L.H. Review of synthetic routes and final forms of integrase inhibitors dolutegravir, cabotegravir, and bictegravir. *Org. Process Res. Dev.* **2019**, *23*, 716–729.
68. Han, J.; Sorochinsky, A.E.; Ono, T.; Soloshonok, V.A. Biomimetic transamination—A metal-free alternative to the reductive amination. application for generalized preparation of fluorine-containing amines and amino acids. *Curr. Org. Synth.* **2011**, *8*, 281–294. [[CrossRef](#)]
69. Wang, X.; Chen, S.; Cui, H.; He, Y.; Zhao, C. Three-step synthetic procedure to prepare dolutegravir, cabotegravir, and bictegravir. *Green Chem. Lett. Rev.* **2022**, *15*, 311–318. [[CrossRef](#)]
70. Shram, M.J.; Spencer, R.H.; Qian, J.; Munera, C.L.; Lewis, M.E.; Henningfield, J.E.; Webster, L.; Menzaghi, F. Evaluation of the abuse potential of difelikefalin, a selective kappa-opioid receptor agonist, in recreational polydrug users. *Clin. Transl. Sci.* **2022**, *15*, 535–547. [[CrossRef](#)] [[PubMed](#)]
71. Wang, X.; Gou, X.; Yu, X.; Bai, D.; Tan, B.; Cao, P.; Qian, M.; Zheng, X.; Wang, H.; Tang, P.; et al. Antinociceptive and antipruritic effects of HSK21542, a peripherally-restricted kappa opioid receptor agonist, in animal models of pain and itch. *Front. Pharmacol.* **2021**, *12*, 773204. [[CrossRef](#)]
72. Schteingart, C.D.; Menzaghi, F.; Jiang, G.; Alexander, R.V.; Sueiras-Diaz, J.; Spencer, R.H.; Chalmers, D.T.; Luo, Z. Synthetic Peptide Amides. WO 2008057608 A2, 15 May 2008.
73. Li, X.; Wan, H.; Dong, P.; Wang, B.; Zhang, L.; Hu, Q.; Zhang, T.; Feng, J.; He, F.; Bai, C.; et al. Discovery of SHR0687, a highly potent and peripheral nervous system-restricted KOR agonist. *ACS Med. Chem. Lett.* **2020**, *11*, 2151–2155. [[CrossRef](#)]

74. Deeks, E.D. Difelikefalin: First approval. *Drugs* **2021**, *81*, 1937–1944. [[CrossRef](#)] [[PubMed](#)]
75. Biron, E.; Chatterjee, J.; Kessler, H. Optimized selective N-methylation of peptides on solid support. *J. Peptide Sci.* **2006**, *12*, 213–219. [[CrossRef](#)] [[PubMed](#)]
76. Gillberg, P.; Graffner, H.; Starke, I. IBAT Inhibitors for the Treatment of Liver Diseases. U.S. Patent 2016/0193277 A1, 7 July 2016.
77. Al-Dury, S.; Wahlström, A.; Wahlin, S.; Langedijk, J.; Elferink, R.O.; Ståhlman, M.; Marschall, H.U. Pilot study with IBAT inhibitor A4250 for the treatment of cholestatic pruritus in primary biliary cholangitis. *Sci. Rep.* **2018**, *8*, 6658. [[CrossRef](#)]
78. Floreani, A. Experimental pharmacological agents for the treatment of primary biliary cholangitis. *J. Exp. Pharmacol.* **2020**, *12*, 643–652. [[CrossRef](#)] [[PubMed](#)]
79. Baumann, U.; Sturm, E.; Lacaille, F.; Gonzalés, E.; Arnell, H.; Fischler, B.; Jørgensen, M.H.; Thompson, R.J.; Mattsson, J.P.; Ekelund, M.; et al. Effects of odeixibat on pruritus and bile acids in children with cholestatic liver disease: Phase 2 study. *Clin. Res. Hepatol. Gas.* **2021**, *45*, 101751. [[CrossRef](#)] [[PubMed](#)]
80. Starke, I.; Graffner, H.; Gillberg, P.G.; Lindqvist, A.M.; Angelin, B. IBAT Inhibitors for Treatment of Metabolic Disorders and Related Conditions. U.S. Patent 2012/0114588 A1, 10 May 2012.
81. Deeks, E.D. Odeixibat: First approval. *Drugs* **2021**, *81*, 1781–1786. [[CrossRef](#)] [[PubMed](#)]
82. Starke, I.; Dahlstrom, M.U.J.; Blomberg, D.; Alenfalk, S.; Skjaret, T.; Lemurell, M. Benzothiazepine and Benzothiadiazepine Derivatives with Ileal Bile Acid Transport (IBAT) Inhibitory Activity for the Treatment Hyperlipidaemia. WO03/022286 A1, 20 March 2003.
83. Handlon, A.L.; Hodgson, G.L.; Hyman, C.E. Hypolipidemic Cyclic Derivatives. WO98/38182, 3 September 1998.
84. Lee, A. Ibrexafungerp: First approval. *Drugs* **2021**, *81*, 1445–1450. [[CrossRef](#)]
85. Ghannoum, M.; Arendrup, M.C.; Chaturvedi, V.P.; Lockhart, S.R.; McCormick, T.S.; Chaturvedi, S.; Berkow, E.L.; Juneja, D.; Tarai, B.; Azie, N.; et al. Ibrexafungerp: A novel oral triterpenoid antifungal in development for the treatment of candida auris infections. *Antibiotics* **2020**, *9*, 539. [[CrossRef](#)] [[PubMed](#)]
86. Apgar, J.M.; Wilkening, R.R.; Parker, D.L., Jr.; Meng, D.; Wildonger, K.J.; Sperbeck, D.; Greenlee, M.L.; Balkovec, J.M.; Flattery, A.M.; Abruzzo, G.K.; et al. Ibrexafungerp: An orally active β -1,3-glucan synthesis inhibitor. *Bioorg. Med. Chem. Lett.* **2021**, *32*, 127661. [[CrossRef](#)] [[PubMed](#)]
87. Apgar, J.M.; Wilkening, R.R.; Parker, D.L., Jr.; Meng, D.; Wildonger, K.J.; Sperbeck, D.; Greenlee, M.L.; Balkovec, J.M.; Flattery, A.M.; Abruzzo, G.K.; et al. MK-5204: An orally active β -1,3-glucan synthesis inhibitor. *Bioorg. Med. Chem. Lett.* **2020**, *30*, 127357. [[CrossRef](#)] [[PubMed](#)]
88. Apgar, J.M.; Wilkening, R.R.; Greenlee, M.L.; Balkovec, J.M.; Flattery, A.M.; Abruzzo, G.K.; Galgoci, A.M.; Giacobbe, R.A.; Gill, C.J.; Hsu, M.J.; et al. Novel orally active inhibitors of β -1,3-glucan synthesis derived from enfumafungin. *Bioorg. Med. Chem. Lett.* **2015**, *25*, 5813–5818. [[CrossRef](#)] [[PubMed](#)]
89. Kollins, S.H.; Braeckman, R.; Guenther, S.; Barrett, A.C.; Mickle, T.C.; Oh, C.; Marraffino, A.; Cutler, A.J.; Brams, M.N. A randomized, controlled laboratory classroom study of serdexmethylphenidate and d-methylphenidate capsules in children with attention-deficit/hyperactivity disorder. *J. Child Adol. Psychop.* **2021**, *31*, 597–609. [[CrossRef](#)] [[PubMed](#)]
90. Guenther, S.; Chi, G.; Mickle, T. Serdexmethylphenidate Conjugates, Compositions and Methods of Use Thereof. WO2019/241020 A1, 19 December 2019.
91. Braeckman, R.; Guenther, S.; Mickle, T.C.; Barrett, A.C.; Smith, A.; Oh, C. Dose Proportionality and steady-state pharmacokinetics of serdexmethylphenidate/dexamethylphenidate, a novel prodrug combination to treat attention-deficit/hyperactivity disorder. *J. Child Adol. Psychop.* **2022**, *32*, 288–295. [[CrossRef](#)] [[PubMed](#)]
92. Mickle, T.; Guenther, S.M.; Chi, G. Compositions Comprising Methylphenidate-Prodrugs, Processes of Making and Using the Same. WO2018/107132 A1, 14 June 2018.
93. Prashad, M.; Har, D.; Repic, O.; Blacklock, T.J.; Giannousis, P. An efficient large scale resolution of (\pm)-threo-methylphenidate hydrochloride (Ritalin[®] hydrochloride). *Tetrahedron Asymmetry* **1999**, *10*, 3111–3116. [[CrossRef](#)]
94. Mahalingam, S.M.; Kularatne, S.A.; Myers, C.H.; Gagare, P.; Norshi, M.; Liu, X.; Singhal, S.; Low, P.S. Evaluation of novel tumor-targeted near-infrared probe for fluorescence-guided surgery of cancer. *J. Med. Chem.* **2018**, *61*, 9637–9646. [[CrossRef](#)]
95. Kularatne, S.A.; Gagare, P.; Noshi, M. Method of Manufacture and Synthesis of Amino Acid Linking Groups Conjugated to Compounds Used for Targeted Imaging of Tumors. WO 2014/149073 A1, 25 September 2014.
96. Tanyi, J.L.; Chon, H.S.; Morgan, M.A.; Chambers, S.K.; Han, E.S.; Butler, K.A.; Langstraat, C.L.; Powell, M.A.; Randall, L.M.; Vahrmeijer, A.L.; et al. Phase 3, randomized, single-dose, open-label study to investigate the safety and efficacy of pafolacianine sodium injection (OTL38) for intraoperative imaging of folate receptor positive ovarian cancer. *J. Clin. Oncol.* **2021**, *39*, 5503. [[CrossRef](#)]
97. Kayki-Mutlu, G.; Aksoyalp, Z.S.; Wojnowski, L.; Michel, M.C. A year in pharmacology: New drugs approved by the US Food and Drug Administration in 2021. *Naunyn-Schmiedeberg's Arch. Pharm.* **2022**, *395*, 867–885. [[CrossRef](#)]
98. Kayki-Mutlu, G.; Michel, M.C. A year in pharmacology: New drugs approved by the US Food and Drug Administration in 2020. *Naunyn-Schmiedeberg's Arch. Pharm.* **2021**, *394*, 839–852. [[CrossRef](#)]
99. Tressaud, A.; Haufe, G. (Eds.) *Fluorine and Health. Molecular Imaging, Biomedical Materials and Pharmaceuticals*; Elsevier: Amsterdam, The Netherlands, 2008.
100. Kirsch, P. *Modern Fluoroorganic Chemistry. Synthesis, Reactivity, Applications*, 2nd ed.; Completely Revised and Enlarged; Wiley-VCH Verlag GmbH & Co. KGaA: Weinheim, Germany, 2013.

101. Ragni, R.; Punzi, A.; Babudri, F.; Farinola, G.M. Organic and organometallic fluorinated materials for electronics and optoelectronics: A survey on recent research. *Eur. J. Org. Chem.* **2018**, *2018*, 3500–3519. [[CrossRef](#)]
102. Bravo, P.; Guidetti, M.; Viani, F.; Zanda, M.; Markovsky, A.L.; Sorochinsky, A.E.; Soloshonok, I.V.; Soloshonok, V.A. Chiral sulfoxide controlled asymmetric additions to C,N double bond. An efficient approach to stereochemically defined α -fluoroalkyl amino compounds. *Tetrahedron* **1998**, *54*, 12789–12806. [[CrossRef](#)]
103. Begue, J.P.; Bonnet-Delpon, D. *Bioorganic and Medicinal Chemistry of Fluorine*; John Wiley & Sons: Hoboken, NJ, USA, 2008.
104. Yamada, T.; Okada, T.; Sakaguchi, K.; Ohfune, Y.; Ueki, H.; Soloshonok, V.A. Efficient asymmetric synthesis of novel 4-substituted and configurationally stable analogs of thalidomide. *Org. Lett.* **2006**, *8*, 5625–5628. [[CrossRef](#)] [[PubMed](#)]
105. Soloshonok, V.A.; Mikami, K.; Yamazaki, T.; Welch, J.T.; Honek, J.F. (Eds.) New Synthetic Directions, Technologies, Materials, and Biological. In *Applications Current Fluoroorganic Chemistry*; ACS Symposium Series 949; American Chemical Society: Washington, DC, USA, 2007.
106. Yerien, D.E.; Barata-Vallejo, S.; Postigo, A. Difluoromethylation reactions of organic compounds. *Chem. Eur. J.* **2017**, *23*, 14676–14701. [[CrossRef](#)] [[PubMed](#)]
107. Soloshonok, V.A.; Cai, C.; Hruby, V.J. A practical asymmetric synthesis of enantiomerically pure 3-substituted pyroglutamic acids and related compounds. *Angew. Chem. Int. Ed.* **2000**, *39*, 2172–2175. [[CrossRef](#)]
108. Han, J.; Nelson, D.J.; Sorochinsky, A.E.; Soloshonok, V.A. Self-disproportionation of enantiomers via sublimation; new and truly green dimension in optical purification. *Curr. Org. Synth.* **2011**, *8*, 310–317. [[CrossRef](#)]
109. Soloshonok, V.A.; Roussel, C.; Kitagawa, O.; Sorochinsky, A.E. Self-disproportionation of enantiomers via achiral chromatography: A warning and extra dimension in optical purifications. *Chem. Soc. Rev.* **2012**, *41*, 4180–4188. [[CrossRef](#)]
110. Sorochinsky, A.E.; Aceña, J.L.; Soloshonok, V.A. Self-disproportionation of enantiomers of chiral, non-racemic fluoroorganic compounds: Role of fluorine as enabling element. *Synthesis* **2013**, *45*, 141–152. [[CrossRef](#)]
111. Sorochinsky, A.E.; Katagiri, T.; Ono, T.; Wzorek, A.; Aceña, J.L.; Soloshonok, V.A. Optical purifications via self-disproportionation of enantiomers by achiral chromatography; case study of a series of α -CF₃-containing secondary alcohols. *Chirality* **2013**, *25*, 365–368. [[CrossRef](#)] [[PubMed](#)]
112. Soloshonok, V.A.; Berbasov, D.O. Self-disproportionation of enantiomers on achiral phase chromatography. One more example of fluorine's magic powers. *Chim. Oggi Chem. Today* **2006**, *24*, 44–47.
113. Nakamura, T.; Tateishi, K.; Tsukagoshi, S.; Hashimoto, S.; Watanabe, S.; Soloshonok, V.A.; Aceña, J.L.; Kitagawa, O. Self-disproportionation of enantiomers of non-racemic chiral amine derivatives through achiral chromatography. *Tetrahedron* **2012**, *68*, 4013–4017. [[CrossRef](#)]
114. Suzuki, Y.; Han, J.; Kitagawa, O.; Aceña, J.L.; Klika, K.D.; Soloshonok, V.A. A comprehensive examination of the self-disproportionation of enantiomers (SDE) of chiral amides via achiral, laboratory-routine, gravity-driven column chromatography. *RSC Adv.* **2015**, *5*, 2988–2993. [[CrossRef](#)]
115. Han, J.; Wzorek, A.; Kwiatkowska, M.; Soloshonok, V.A.; Klika, K.D. The self-disproportionation of enantiomers (SDE) of amino acids and their derivatives. *Amino Acids* **2019**, *51*, 865–889. [[CrossRef](#)]
116. Hosaka, T.; Imai, T.; Wzorek, A.; Marcinkowska, M.; Kolbus, A.; Kitagawa, O.; Soloshonok, V.A.; Klika, K.D. The self-disproportionation of enantiomers (SDE) of α -amino acid derivatives; facets of steric and electronic properties. *Amino Acids* **2019**, *51*, 283–294. [[CrossRef](#)]
117. Wzorek, A.; Sato, A.; Drabowicz, J.; Soloshonok, V.A.; Klika, K.D. Remarkable magnitude of the self-disproportionation of enantiomers (SDE) via achiral chromatography; application to the practical-scale enantiopurification of β -amino acid esters. *Amino Acids* **2016**, *48*, 605–613. [[CrossRef](#)]
118. Han, J.; Kitagawa, O.; Wzorek, A.; Klika, K.D.; Soloshonok, V.A. The self-disproportionation of enantiomers (SDE): A menace or an opportunity? *Chem. Sci.* **2018**, *9*, 1718–1739. [[CrossRef](#)]
119. Han, J.; Soloshonok, V.A.; Klika, K.D.; Drabowicz, J.; Wzorek, A. Chiral sulfoxides: Advances in asymmetric synthesis and problems with the accurate determination of the stereochemical outcome. *Chem. Soc. Rev.* **2018**, *47*, 1307–1350. [[CrossRef](#)]
120. Soloshonok, V.A.; Wzorek, A.; Klika, K.D. A question of policy: Should tests for the self-disproportionation of enantiomers (SDE) be mandatory for reports involving scalemates? *Tetrahedron Asymmetry* **2017**, *28*, 1430–1434. [[CrossRef](#)]
121. Han, J.; Wzorek, A.; Klika, K.D.; Soloshonok, V.A. Recommended tests for the self-disproportionation of enantiomers (SDE) to ensure accurate reporting of the stereochemical outcome of enantioselective reactions. *Molecules* **2021**, *26*, 2757. [[CrossRef](#)] [[PubMed](#)]
122. Han, J.; Dembinski, R.; Soloshonok, V.A.; Klika, K.D. A call for a change in policy regarding the necessity for SDE tests to validate the veracity of the outcome of enantioselective syntheses, the inherent chiral state of natural products, and other cases involving enantioenriched samples. *Molecules* **2021**, *26*, 3994. [[CrossRef](#)] [[PubMed](#)]